Postharvest Biology and Technology, Volume 205, November 2023, Article number 112532
DOI:10.1016/j.postharvbio.2023.112532

Cultivar differences in the hormonal crosstalk regulating apple fruit development and ripening: relationship with flavour components and postharvest susceptibility to *Penicillium expansum*

Pablo Fernández-Cancelo[1], Gemma Echeverria[1], Neus Teixidó[1], M. Carmen Alamar[2] and Jordi Giné-Bordonaba[1*]

[1]*Postharvest Programme, Institute of Agrifood Research and Technology (IRTA), Edifici Fruitcentre, Parc Agrobiotech Lleida, Parc de Gardeny, 25003 Lleida, Spain.*

[2]*Plant Science Laboratory, Cranfield University, Cranfield MK43 0AL United Kingdom*

Abstract

The hormonal interplay during the on-tree development and ripening of three apple cultivars with known differences in their postharvest ripening patterns was studied, at the biochemical and targeted gene expression level, along with characterizing the changes in main sugars, acids, phenylpropanoids and volatile organic compounds (VOCs). Our findings suggest that in 'Royal Gala' and 'Opal®' apples, a peak in indole 3-acetic acid (IAA) seems necessary to activate ethylene metabolism, being its intensity proportional to the ethylene production. The interplay between IAA and ethylene appears to be mediated by *MdARF5*, responsible for activating the expression of *MdACS3* and triggering ethylene metabolism. On the other hand, the lack of ethylene production observed in 'Granny Smith' apples was likely related to the absence of an IAA peak and possibly caused by the over activation of IAA conjugation mechanisms leading to a greater accumulation of IAA inactive conjugates such as indole-3-acetyl-aspartate (IAAsp). Abscisic acid (ABA) accumulation was only observed in cultivars with the ability to accumulate sucrose and produce ethylene, suggesting a possible crosstalk among those hormones and sucrose in orchestrating apple on-tree ripening. While differences in hormone levels among cultivars led to noticeable differences in some specific VOCs, no evident associations were found between hormone changes and the accumulation or degradation of monosaccharides, organic acids or phenolic compounds during fruit development and ripening. Likewise, no clear relationship was found between the fruit susceptibility to blue mould and hormonal levels yet certain specific biochemical compounds (i.e., procyanidins and sucrose) could be acting as a source of resistance or susceptibility, respectively, to blue mould development. Overall, understanding the cultivar specific hormonal regulation of apple on-tree ripening provides valuable insights to optimize fruit quality at the time of harvest as well as to develop strategies for improved postharvest management.

Keywords: Abscisic acid (ABA), blue mould, ethylene, indole 3-acetic acid (IAA), *MdARF5,* procyanidin, sucrose

Published by Elsevier. This is the Author Accepted Manuscript issued with: Creative Commons Attribution Non-Commercial No Derivatives License (CC:BY:NC:ND 4.0).
The final published version (version of record) is available online at DOI:10.1016/j.postharvbio.2023.112532. Please refer to any applicable publisher terms of use.

Introduction

Ethylene plays a crucial role in triggering the physiological changes during the ripening of climacteric fruit, including apples (Bapat et al., 2010). However, recent evidence suggests that not only ethylene but other hormones, such as indole 3-acetic acid (IAA) and abscisic acid (ABA), are also involved in the ripening process (Ji and Wang, 2021). In climacteric fruit, changes associated to ripening, including softening and changes in taste and aroma, mainly occur when ethylene transits from the autoinhibitory phase (system 1) to the autocatalytic phase (system 2). This transition is characterized by a burst in the ethylene production and is associated to rapid changes in specific quality parameters (Sfakiotakis and Dilley, 1973; Tan et al., 2013). In the specific case of apple, a model fruit for climacteric ripening besides tomato, the transition from system 1 to system 2 is paralleled by changes in the expression of ethylene response factors (*MdERFs*) and paralogous genes encoding for the enzymes involved in the last steps of the ethylene biosynthesis pathway, 1-aminocyclopropane-1-carboxylic (ACC) synthase (ACS) and ACC oxidase (ACO) (i.e. *MdACS1* and *MdACO1*; Pattyn et al., 2021).

During the autoinhibitory phase (system 1), the low ethylene biosynthesis is sustained by the expression of *MdACS6* and *MdACS3* as well as *MdERF2*, the latter inhibiting the expression of *MdACS1* and *MdACO1* (Li et al., 2015; T. Li et al., 2016; Tan et al., 2013). While the real driver of the transition from system 1 to system 2 is not yet fully understood, recent studies in apples suggest that such transition may be mediated by auxins and auxin response factor 5 (*MdARF5)*, both being able to inhibit the expression of *MdERF2* while concomitantly activating the expression of *MdACO1* (Yue et al., 2020). Likewise, auxins have also been described as key regulators of ethylene biosynthesis in other climacteric fruit species including tomato (Fernie and Alseekh, 2018), peach (Tatsuki et al., 2013) and pear (Lindo-García et al., 2020). ABA, on the other hand, has

also been pointed out to trigger ethylene production in climacteric fruit since an increase in endogenous ABA levels prior to the ethylene burst was observed in pear (Lindo-García et al., 2020) and peach (García-Pastor et al., 2021), while exogenous ABA treatments generally induced ethylene production in apple and tomato (Vendrell and Buesa, 1989; Zhang et al., 2009). Recently, results from a more comprehensive study comparing attached and detached apple ripening revealed that ABA may not be required to initiate ethylene production (Fernández-Cancelo et al., 2022b), but rather involved in the ethylene signalling cascade, hence in agreement to that suggested for other climacteric fruit (i.e. figs; Qiao et al., 2021).

Nowadays, however, strong evidence suggest that ripening is regulated through a complex hormonal crosstalk rather than by the action of individual hormones. A good example is the synergistic interaction between ABA and ethylene, which promotes softening in bananas and apples (Fernández-Cancelo et al., 2022b; Jiang et al., 2000) and enhances the biosynthesis of volatile esters in apples (Wang et al., 2018) or the cooperation between auxin and ethylene being tightly involved in the biosynthetic regulation of some VOCs in tomatoes (Tobaruela et al., 2021). Not only hormones, but also other compounds including sugars and reactive oxygen species (ROS) have been proposed to play an essential role in triggering fruit ripening (Decros et al., 2019; Durán-Soria et al., 2020; Vall-llaura et al., 2022a), while some phenolic compounds can have the opposite effect (Xi et al., 2016). Sucrose and ROS, for instance, may promote the autocatalytic burst of ethylene production in pear (Lindo-García et al., 2019) and tomato (Kumar et al., 2016), whereas certain phenolic compounds may inhibit ripening in apple (Xi et al., 2016) and peach (Vall-llaura et al., 2022a).

Interestingly, ROS and certain hormones, alone or in combination, not only affect fruit ripening but also can influence the fruit susceptibility/resistance to certain postharvest

rots (reviewed by Vall-llaura et al., 2022b). This said, little information is currently available regarding the role of specific hormones or ripening-related biochemical compounds on the apple susceptibility or resistance to the main postharvest disease of apples – the blue mould caused by *Penicillium expansum*.

Accordingly, the main objective of our study was to investigate, at both the biochemical and targeted gene expression level, the interplay among ethylene, IAA, and ABA during the development and ripening of different apple cultivars, as well as their possible involvement in regulating the content of flavour and ripening-related compounds such as sugars, organic acids, and VOCs. Moreover, given the potential participation of the targeted biochemical components in the fruit defence against postharvest rots, the secondary objective of our investigation was to elucidate whether hormonal or biochemical changes during apple growth and ripening influence the fruit's susceptibility to *P. expansum* infection.

Material and methods

Fruit material and experimental design

In 2021, three apple cultivars – 'Royal Gala', 'Granny Smith', and 'Opal®' – were chosen to investigate their development and ripening on the tree. These cultivars were selected based on their commercial relevance in the Ebro Valley (Spain) as well as their distinct ripening patterns and ethylene production capacities. Specifically, 'Royal Gala' apples can produce ethylene in the final stages of on-tree ripening, while 'Granny Smith' apples maintained low ethylene levels even at harvest (Busatto et al., 2021; Favre et al., 2022). On the other hand, the ripening pattern of 'Opal®' apple, a novel commercial cultivar, has not been investigated yet.

The study was conducted in a commercial orchard located in Alcarràs, Lleida, Spain. The analyzed apple cultivars had similar flowering times, with a maximum difference of 5 days among them. 'Opal®' apples initiated their blooming period 5 days earlier than the 'Royal Gala' and 'Granny Smith' cultivars, which had the same flowering times. 'Opal®' and 'Granny Smith' apples were studied at 6 sampling points, while 'Royal Gala' apples were sampled at 4 sampling points (Table 1). The first four sampling points were performed simultaneously for all three cultivars every 25-30 days. The sampling point S4 corresponded to 125 DAFB for 'Royal Gala' and 'Granny Smith' and 130 DAFB for 'Opal®'. Since 'Granny Smith' and 'Opal®' apples required more time to ripen, two additional sampling points were included. The fifth sampling point (S5) corresponded to 151 DAFB for 'Granny Smith' and 156 DAFB for 'Opal®', while the sixth sampling point (S6) and CHD were set at 173 DAFB (September 27th) for 'Opal®' and 172 DAFB (October 1st) for 'Granny Smith' (Table 1). To conduct our analysis, twenty trees were randomly selected for each cultivar, and apples were collected at the same canopy height (mid canopy). For each cultivar and sampling point, 20 fruit were used for quality evaluations and another 20 fruit were used for *P. expansum* inoculation assays. Ethylene measurements were performed using four replicates per cultivar of about 1 kg of fruit per replicate. Additionally, for each cultivar and sampling point, 40 apples (10 apples per replicate and 4 replicates) were peeled and the pulp was snap-frozen in liquid nitrogen, ground and stored at −80°C until further biochemical analysis. A portion of the frozen and ground sample was freeze-dried for 72 hours to conduct hormones and phenolic compounds analyses.

Fruit quality evaluation

Fruit diameter was measured on 20 fruit per sampling point and cultivar combination, whereas firmness and starch index were only measured at two sampling points: at the commercial harvest date (CHD) and at the immediately preceding sampling point, as described by Fernández-Cancelo et al. (2021). The same fruits used for firmness measurements were used to produce four juices (5 fruit per juice, considering juices as replicates) required to determine the Soluble Solids Content (SSC) and Total Titratable Acidity (TTA) as described by Giné-Bordonaba et al. (2016).

Ethylene production and ethylene-related metabolites and enzymes

At each sampling point, four replicates per cultivar of about 1 kg of fruit per replicate were placed in an acclimatized chamber at 20 °C in 3.8 L flasks sealed with a silicon septum. After 2 h incubation, ethylene production (nmol kg^{-1} s^{-1}) was measured by taking 1 mL of gas from the headspace of the flask with a syringe and injected into a gas chromatograph (GC) Agilent 6890 (Agilent Technologies, Santa Clara, CA, USA) fitted with a flame ionization detector (FID) detector and an alumina column F1 80/100 (2 m × 1/8″ OD × 2.1 mm ID, Teknokroma, Barcelona, Spain) as previously described by Lindo-García et al., (2020). Determination of enzymatic activities (ACO and ACS) and metabolites levels (ACC and MACC) involved in ethylene metabolism were carried out on apple flesh samples according to Bulens et al. (2011) with some modifications (Lindo-García et al., 2020).

Hormonal profiling

Endogenous phytohormones were extracted by mixing 100 mg of the freeze-dried apple pulp samples with 5 mL methanol:water:formic acid, 60:35:5 (v/v/v) and 50 µL of

Deuterium-labelled internal standards (100 ng mL^{-1}). The mixture was vortexed for 2 min at 2,000 rpm, kept in ice and dark for 20 min and centrifuged at 4,500 g for 10 minutes at 4ºC. The supernatant was recovered and freeze-dried overnight. The freeze-dried samples were dissolved with 0.5 mL methanol:water:formic acid 1:9:0.1 solution (v/v/v) containing ammonium formate (1mM), vortexed at 2,000 rpm for 3 min and centrifuged at 4,500 g for 10 minutes at 4ºC. The supernatant was collected and filtered through 0.22 µm Polytetrafluoroethylene (PTFE) filter into silanized amber vials. Hormones separation and identification were carried out according to Collings et al., (under publication). Briefly, 10 µL of extract were injected on a LC–MS/MS instrument with an Agilent 1200 series High Performance Liquid Chromatography (HPLC) system (Agilent, Berkshire, United Kingdom) coupled with a Q-Trap 6500 mass spectrometer (AB Sciex, Framingham, MA, USA), and equipped with a Hypersil GOLD C18 (50 x 2.1 mm, 1.9 µm) (ThermoFisher Scientific, Waltham, MA, USA) held at 30 °C. Separation was carried out at a flow rate of 0.4 mL min^{-1} using a mobile phase consisting in a mixture of 0.1% formic acid and ammonium formate (1mM) in water (A) and 0.1% formic acid and ammonium formate (1mM) in methanol (B), using an increasing gradient of B (5 % for 1 min, 40 % at 5 min, 95 % at 6.5 min which was hold for 1 min, then back to 5% at 8.5). The concentration of the plant hormones was quantified using a 10-point calibration curve ranging from 1 ng mL^{-1} to 250 ng mL^{-1} for each analysed phytohormone, and it was expressed in µg kg^{-1} dry weight (DW). Deuterated and non-deuterated ABA metabolites: (+)-ABA-glucose ester (ABA-GE), (−)-phasic acid (PA), (−)-dihydrophaseic acid (DPA), (−)-neo-PA, and (±)-7'-OH-hydroxy-ABA were purchased from the National Research Council of Canada - Plant Biotechnology Institute (Saskatoon, SK, Canada); (±)-ABA was obtained from Sigma-Aldrich (Darmstadt, Germany); and the auxins Indole-3-acetic

acid (IAA) and indole-3-acetyl-aspartic acid (IAAsp) were purchased from OlChemIm, Olomouc, Czech Republic.

Sugars and acids quantification

The protocols described by Fernández-Cancelo et al., (2021) were used for extracting malic acid and sugars (sucrose, glucose, and fructose) from 0.5 g of frozen pulp tissue and using 1 mL of extraction solvent. Ascorbic acid (AsA) and dehydroascorbic acid (DHA) were extracted from 2.5 g of frozen pulp tissue mixed with 5 mL of metaphosphoric acid suspension (3% metaphosphoric acid, 8% acetic acid) and quantified via HPLC as previously described (Fernández-Cancelo et al., 2021).

Phenolic compounds identification and quantification

Phenolic compounds were extracted following the protocol described by Fernández-Cancelo et al. (2022a), with some modifications. Briefly, 50 mg of freeze-dried pulp tissue were mixed with 1 mL of 79.5% (v/v) methanol and 0.5% (v/v) HCl in Milli-Q water, incubated in a water batch for 30 min at 35 ºC, and centrifugated at 20,000 *g* for 30 min at room temperature. The extract was filtered through 0.22 µm PTFE filter and injected (10 µL) on an Agilent 1200 liquid chromatograph (Agilent Technologies, Santa Clara, CA, USA) fitted with an Eclipse XDB-C18 column (250 x 4.6 mm, 5.0 µm) (Agilent Technologies, Santa Clara, CA, USA). Phenolic compounds were separated and identified according to Anastasiadi et al. (2017) methodology. Quantification was performed using calibration curves prepared with standard stock solutions of procyanidin B1, procyanidin B2, chlorogenic acid, catechin, epicatechin and phloretin-2'-O-glucoside, and their concentrations were expressed as g kg^{-1} DW. When no commercial standard

was available, detected phloretin derivatives were quantified using phloretin-2'-O-glucoside standard curve.

Volatile profiling

Headspace solid-phase microextraction (HS-SPME) was performed for extracting and determining the volatile organic compounds (VOCs). Based on previous protocols (Yang et al., 2022), the extraction of volatile compounds was performed by mixing 3 g of frozen apple pulp, 1.25 g NaCl, 3 mL Milli-Q water and 20 µL internal standard (3-nonanone/diethyl ether = 1:10000, v/v) in a 28 mL screw-capped vial. Immediately, the vial was sealed, and the suspension vortexed and incubated in an ultrasonic bath (JP Selecta, Abrera, Barcelona, Spain) for 10 min to facilitate the release of the volatile compounds. Afterwards, the headspace vial was equilibrated at 40 ºC for 15 min on a metal heating agitation platform, and a SPME fibre coated with 50/30 µm thickness of divinylbenzene/carboxen/polydimethylsiloxane (DVB/CAR/PDMS, Supelco, Bellefonte, PA, USA) was inserted into the headspace with continuous heating and agitation (200 rpm) for 10 min to adsorb the VOCs. Then, the fibre was introduced into the heated injector port of the chromatograph for desorption at 250 ºC for 5 min. The volatile compounds were analysed with an Agilent 7890A gas chromatograph (GC) coupled to an Agilent 5977A Mass Selective Detector (MSD) (Agilent Technologies, Santa Clara, CA, USA), equipped with a 50 m × 0.20 mm × 0.33 µm HP-FFAP capillary column (Agilent Technologies, Santa Clara, CA, USA). Helium was circulated as the carrier gas with a flow of 1.0 mL min^{-1} in a splitless mode. The initial oven temperature was kept at 40 ºC for 3 min, then increased to 220 ºC at a rate of 4 ºC min^{-1}, and finally held for 5 min. Mass spectra were operated in electron ionization mode of 70 eV with the scan range from m/z 30 to 350. Identification of VOCs was based on mass spectra

matching with the database of National Institute of Standards and Technology (NIST, 2011). Quantification was carried out by the internal standard method where the concentration of each volatile compound was relativized to the concentration of 3-nonanone.

RNA isolation and qPCR analysis

RNA extraction, cDNA synthesis and gene expression analysis were performed following the protocols described by Fernández-Cancelo et al. (2022a). Primers used in this study were retrieved from the literature or designed *de novo* when indicated (Table S1). Relative gene expression was expressed as Mean Normalized Expression (MNE) according to previous studies (Muller et al., 2002) using *Md8283* as a reference gene.

P. expansum inoculation

Conidial suspensions of *P. expansum* were prepared to obtain 10^5 conidia mL^{-1} following the method described by Vilanova et al., (2014). Immediately after harvest at each developmental stage (sampling point), including the commercial harvest of 'Royal Gala' at S4 and 'Granny Smith' and 'Opal®' at S6, twenty apples per cultivar were wounded with a nail (1 mm wide and 2 mm deep) to produce an injury on the equatorial part and expose the pulp avoiding the possible influence of peel on the rot development tacking into account that *P. expansum* is an injury pathogen. The wounds were inoculated with 15 µL of an aqueous suspension of *P. expansum* and fruit were allowed to dry at room temperature. Then, inoculated apples were incubated at 20 °C and 85% relative humidity and rot lesion diameters (severity) were determined 10 days after postharvest inoculation.

Statistical data analysis

Biochemical and gene expression data were subjected to analysis of variance (ANOVA) test using the R 'agricolae' package. Least significant difference values (LSD, p=0.05) for the interaction cultivar × sampling point were calculated for mean separation, for all cultivars from S1 to S4 (LSD1) and for 'Opal®' and 'Granny Smith' apples from S1 to S6 (LSD2), using critical values of t for two-tailed tests. Rot severity data were also subjected to analysis of variance (ANOVA) test when comparison was made among three cultivars at each sampling point from S1 to S4 and to Students' t-test when 'Opal®' and 'Granny Smith' were compared at S5 and S6. When the analysis was statistically significant, Tukey's HSD test at the level $p \leq 0.05$ was performed for comparison of means for among cultivars at each developmental stage. Pearson's correlation matrix ($p \leq 0.05$) was done using the R 'corrplot' package. A hierarchical cluster analysis (HCA) dendrogram was done applying Ward method of minimum variance to stablish a relationship among the VOCs detected in the studied cultivars and sampling points. Partial least square (PLS) regression models were used to correlate biochemical composition, gene expression and ethylene production (as X variables or explanatory variables) with *P. expansum* severity as response variable (Y). The Non-Linear Iterative Partial Least Squares (NIPALS) algorithm with four factors was used for estimating the model parameters. Data for PLS model were centred and weighed by the inverse of the standard deviation of each variable to avoid dependence on measured units. JMP software version 16.0.0 (SAS Institute Inc. Cary, NC, USA) was used to perform the HCA and PLS analysis.

Results

Fruit quality parameters

'Royal Gala', 'Opal®' and 'Granny Smith' apples presented the same growth dynamics, increasing their diameters from 38 mm at the first sampling point (S1) to 73 mm at S4, when 'Royal Gala' apples were harvested (Figure S1). During the first four sampling points, fruit growth rate slowed down from an average of 0.6 mm day^{-1} during the period S1 to S2 to 0.3 mm day^{-1} in the period from S3 to S4. Growth continued thereafter in 'Opal®' and 'Granny Smith' with a growth rate below 0.3 mm day^{-1} while no growth was observed in 'Opal®' in the period from S5 to S6. At the commercial harvest date (CHD, sampling point S6), 'Opal®' and 'Granny Smith' apples reached a final size of 78 mm and 82 mm, respectively (Figure S1). Quality parameters were analysed both at harvest and at the preharvest sampling point (Table 2). 'Royal Gala' apples showed the greatest decrease in firmness (30 N) and starch index (6 units), while 'Granny Smith' and 'Opal®' showed the same decrease in firmness (10 N) and starch index (2 units) among the last two sampling points. This said, at the CHD, firmness was highest in 'Granny Smith' (79 N), followed by 'Royal Gala' (76 N) and 'Opal®' (74N) while starch index was highest in 'Opal®' (8 units), followed by 'Royal Gala' (7 units) and 'Granny Smith' (5 units). Differences in SCC and TTA were also observed among cultivars at harvest, being 'Granny Smith' the cultivar with higher TTA (5.6 g L^{-1}) and lower SCC (11.0 ºBrix) levels, whereas 'Opal®' presented the highest SCC (14.5 ºBrix) values (Table 2).

Ethylene metabolism

Ethylene metabolism was strongly dependent on the cultivar, particularly during the latter stages of fruit development (Figure 1). During the first three developmental stages, ethylene production remained below $2 \cdot 10^{-4}$ nmol kg^{-1} in all cultivars, with 'Granny

Smith' remaining within these values even in successive stages (Figure 1D). In turn, 'Opal®' and 'Royal Gala' were able to produce ethylene in the final developmental stages, but with substantial different behaviours. 'Royal Gala' showed a sharp increase in ethylene only at harvest (S4), reaching $9 \cdot 10^{-3}$ nmol kg^{-1}, whereas 'Opal®' reached a peak of ethylene prior to harvest (S5) ($3 \cdot 10^{-3}$ nmol kg^{-1}) followed by a 2-fold reduction at the time of harvest (S6). Differences among cultivars were also observed in the enzymes involved in ethylene biosynthesis. ACO showed the same evolution as ethylene (Figure 1C), reaching the maximum activity at S4 in 'Royal Gala' (0.9 nmol kg^{-1} s^{-1}) and at S5 in 'Opal®' (0.3 nmol kg^{-1} s^{-1}). Differences in ACS activity, ACC and MACC levels were less significant among cultivars given their generally low levels during on-tree development (Figures 1A, 1B and 1E). However, an upward trend was observed in ACS activity (Figure 1A) and ACC levels (Figure 1B) during fruit development, especially in 'Royal Gala'. The highest ACS activity was detected in 'Royal Gala' at S4 (0.003 nmol kg^{-1} s^{-1}), followed by 'Opal®' at S5 ($2.8 \cdot 10^{-3}$ nmol kg^{-1} s^{-1}) whereas the ACS activity remained below $2.0 \cdot 10^{-3}$ nmol kg^{-1} s^{-1} during all fruit development in 'Granny Smith' (Figure 1A). ACC levels reached a peak of 133 nmol kg^{-1} at S3 in 'Royal Gala' whereas the maximum ACC concentration was reached at S5 in 'Opal®' (96 nmol kg^{-1}) and at S6 in 'Granny Smith' (71 nmol kg^{-1}) (Figure 1B). MACC only differed at S1 when 'Opal®' and 'Granny Smith' showed 1.7-fold higher levels if compared to 'Royal Gala' (Figure 2D). However, during the last stages of fruit development MACC levels remained to similar levels (*ca*.300 nmol kg^{-1}) in the three studied cultivars.

Differences among apple cultivars were also observed in the genes involved in ethylene biosynthesis and signalling, except for *MdERF1* (Figure S2). An increase in the expression of *MdACS3* and *MdACO1* was observed in the last developmental stages in 'Royal Gala' and 'Opal®', whereas the expression of these genes remained low in

'Granny Smith' (Figures S2B and S2C). In contrast, the expression of *MdACS1* remained low and practically unchanged during fruit development in the three studied cultivars (Figure S2A). However, it is important to notice that in 'Granny Smith' apples, the expression of *MdACS1* was 10-fold greater than that observed for *MdACS3* during the initial fruit developmental stages and that this specific gene remained as the most expressed *MdACS* paralogue in 'Granny Smith' even at the time of commercial harvest (Figures S2A and S2B). *MdERF1* was highly expressed in all cultivars (Figure S2E), showing a similar increasing trend in all three cultivars until it reached a peak at stages S4 for 'Gala' and 'Opal®' and S5 for 'Granny Smith', followed by a decrease in 'Opal®' and 'Granny Smith'. In turn, *MdERF2* and *MdERF3* presented low expression levels and remained practically unchanged during development (Figures S2F and S2G), except for an increase observed in the expression of *MdERF2* at S5 and S6 in 'Opal®' and in *MdERF3* at S2 in 'Granny Smith'. The expression of the ethylene receptor *MdETR1* remained unchanged in the three studied cultivars except in Gala at S4, when transcription increased 2.2-fold (Figure S2H).

Auxin and ABA metabolism

Differences among cultivars were also observed in the evolution of indole-3-acetic acid (IAA) and indole-3-acetyl-aspartate (IAAsp), the IAA-amide conjugate (Figure 2). IAA levels remained below 0.5 μg kg^{-1} during fruit development except in 'Royal Gala' at S3 and in 'Opal®' at S5 and S6 when levels rose to 0.9 μg kg^{-1} and 0.6 μg kg^{-1}, respectively (Figure 2A). IAAsp levels declined in 'Royal Gala' from 0.18 ng kg^{-1} at S1 to 0.03 ng kg^{-1} at S4 whereas IAAsp remained unchanged and below 0.06 ng kg^{-1} 'Opal®'. In turn, 'Granny Smith' showed a peak of IAAsp at S1 and S5, reaching levels of 0.14 ng kg^{-1} in both points (Figure 2B) and being 3 to 4-fold higher than that observed in the other

cultivars at S4 and S5. Accompanying the differences in the auxin levels, differences in the expression of auxin response factors (ARFs) among cultivars were especially pronounced in the last stages of fruit development (Figure S3). The expression of *MdARF5* remained low and unchanged in 'Granny Smith' (Figures S3C) whereas the transcription of *MdARF2* and *MdARF4* tended to be higher in 'Granny Smith' in the later sampling points (S4 to S6) if compared with the other cultivars (Figures S3A and S3B). In turn, an increase in the expression of *MdARF5* was only observed in 'Royal Gala' and 'Opal®' at S4, and it remained high in 'Opal®' during the last stages of development (Figure S3C).

Overall, the major concentration differences in ABA and its catabolites were found in the later stages of development (S4 to S6) and, to a lesser extent, at the first sampling point (S1) (Figure 3). ABA and its catabolites remained low and unchanged in 'Granny Smith' from S2 to S6, whereas a sharp accumulation was observed in 'Royal Gala' at S4 and in 'Opal®' at S4 and thereafter. ABA presented a similar evolution profile in 'Royal Gala' and 'Opal®', reaching the maximum concentration (150 μg kg^{-1}) at S4 and S5, respectively (Figure 3B). The other ABA catabolites followed the same trend as observed for ABA except for DPA and ABA-GE (Figures 3E and 3F). Only 'Opal®' apples presented an accumulation of ABA-GE in the last steps of fruit development, increasing from 10 μg kg^{-1} at S3 to 120 μg kg^{-1} at S6 (Figure 3E).

Sugars, acids and phenolic compounds content

The biochemical compounds that showed the greatest differences in their behaviour among the cultivars were glucose, sucrose, and malic acid, whereas the evolution of fructose and phenolic compounds along fruit development was barely affected by the cultivar (Figures 4 and 5). Glucose raised from 9 g kg^{-1} to 15 g kg^{-1} during 'Granny Smith'

development. In turn, glucose levels in 'Royal Gala' and 'Opal®' decreased from 11 g kg^{-1} at S1 to 4 and 6 g kg^{-1}, respectively. Sucrose levels followed an upward trend from less than 10 g kg^{-1} in all cultivars at S1 to 15 g kg^{-1} in 'Granny Smith' at S6, 43 g kg^{-1} in 'Royal Gala' at S4 and 32 g kg^{-1} in 'Opal®' at S5 and S6 (Figure 4E). Malic acid showed a decrease in 'Opal®' and 'Granny Smith' from 16 g kg^{-1} at S1 to 7 g kg^{-1} at S6, whereas malic acid levels in 'Royal Gala' remained unchanged around 5 g kg^{-1} between S2 and S4 (Figure 4B).

The levels of the identified seven phenolic compounds also exhibited a general decreasing trend in all cultivars, characterised by a sharp reduction in the transition from S1 to S2 (Figure 5). Chlorogenic acid was the most abundant phenolic compound found among the cultivars, with 'Royal Gala' presenting the highest levels ranging from 4.8 g kg^{-1} at S1 to 0.7g kg^{-1} at S4, while 'Opal®' exhibited the lowest levels ranging from 1.5 to 0.2 g kg^{-1}, which matched with the levels in 'Granny Smith' at S6 (Figure 5C). In contrast, epicatechin (Figure 5E), the second most abundant phenolic compound and the main flavanol, presented the lowest levels in 'Royal Gala' (decreasing from 2.0 g kg^{-1} at S1 to 0.2 g kg^{-1} at S4), while 'Opal®' showed the highest levels, especially in the early stages (2.6 g kg^{-1} at S1). Procyanidin B1 and procyanidin B2 showed a smoother decline during development but differences in their levels were more pronounced among the cultivars if compared to other phenolic compounds (Figures 5F and 5G). 'Granny Smith' presented the highest levels of procyanidin B1 (decreasing from 0.10 g kg^{-1} during the first three sampling points to 0.06 g kg^{-1} at S6), while the levels in 'Royal Gala' and 'Opal®' were 2-fold lower than those in 'Granny Smith' from S3 to S6 (Figure 5F). Procyanidin B2 levels in 'Granny Smith' decreased from 0.82 g kg^{-1} at S1 to 0.20 g kg^{-1} at S6, while 'Royal Gala' and 'Opal®' had a similar progression but with levels 3-fold and 1.5-fold lower, respectively, during most of the development period (Figure 5G). Dihydrochalcones

exhibited the lowest concentration in the pulp among the phenolic compound classes, with levels of phloretin 2'-O-glucoside and phloretin 2'-O-xylosyl-glucoside lower than 0.1 g kg^{-1} from S3 and beyond in all cultivars (Figures 5A and 5B). Flavonols or anthocyanins were not detected in the pulp any of the three cultivars studied.

VOCs levels

Developmental stage and cultivar had a strong influence in the levels of VOCs (Figure 6). Aldehydes were the predominant group of VOCs in the early stages of development in both 'Granny Smith' and 'Royal Gala' apples, being more than 80% of total VOCs emitted in 'Granny Smith' and ranging between 60-80% in 'Royal Gala'. In contrast, the contribution of aldehydes to the total VOCs in 'Opal®' was found to be around 40-60% at earlier developmental stages. Aldehydes remained the main group of VOCs in 'Granny Smith' at the last developmental stages, whereas a strong increase of esters, alcohols and volatile phenylpropanoids levels was observed in 'Royal Gala' at S4 and 'Opal®' at S5 and S6 (Figure 6). Alcohols and esters levels were around 26 µg kg^{-1} and 200 µg kg^{-1} in 'Royal Gala' at S4 and 'Opal®' at S5, respectively, and continued to rise until 65 µg kg^{-1} and 515 µg kg^{-1} in 'Opal®' at S6 (Figures 6A and 6C), mainly favoured by the biosynthesis of hexyl acetate, 2-methylbutyl acetate, 1-hexanol and 2-ethyl hexanol (Table S2). Consequently, esters became the main group of VOCs emitted in 'Royal Gala' at S4 and 'Opal®' at S6, representing 60% and 78% of total VOCs. In the same developmental stages (S4 or S6), an increase of phenylpropanoids levels were observed in 'Royal Gala' (27 µg kg^{-1}) and 'Opal®' (13 µg kg^{-1}), respectively, (Figure 6D) driven by the rise in estragole levels (Table S2).

Cultivar susceptibility to 'P. expansum'

Apple susceptibility to blue mould, measured as the rot diameter after inoculation, increased during fruit development in the three studied cultivars (Figure 7A). In the two first sampling points (S1 and S2), lesion diameters remained below 0.5 cm in all cultivars, being 'Royal Gala' the least susceptible cultivar to *P. expansum* infection. A strong increase in the susceptibility was observed in 'Opal®' apples at S3, reaching 4.3 cm of rot diameter whereas 'Royal Gala' and 'Granny Smith' apples were more resistant to the pathogen, with 1.5 and 1.3 cm rot diameters, respectively, at the same developmental stage. 'Royal Gala' apples reached the maximum rot diameter (4.6 cm) at S4 whereas 'Granny Smith' apples only reached their highest (4.4 cm) at S6, similar to the rot diameter observed in 'Opal®' at S6 (4.5 cm). The PLS model pointed out that phenolics compounds, specially procyanidin B1, and some VOCs like 6-methyl-5-hepten-2-one and 4-penten-1-yl acetate had a negative effect in the development of blue mould, whereas fructose and sucrose were positively associated to *P. expansum* growth (Figure 7C and 7D).

Discussion

An intermediate transition system between ethylene system 1 and 2 arises at the last stages of apple developmental.

Ethylene is well known to play a crucial role in the biochemical changes associated with apple ripening (Yang et al., 2013) and pome fruit development (Giné-Bordonaba et al., 2019; Lindo-García et al., 2020). The results from our study reveal that ethylene biosynthesis and to a lesser extent ethylene perception and signalling strongly differed among the studied cultivars throughout fruit development and ripening (Figure 1), despite all cultivars displaying similar growth dynamics (Figure S1) and fruit being harvested, at

the last stage, using similar quality criteria (firmness between 70 and 80 N and starch index of 5 or higher) (Table 2).

At the biosynthetic level, the differences among cultivars were regulated enzymatically since ethylene was strongly positively correlated with the enzymatic activity of ACS and particularly ACO (Figure S4). Indeed, ACO seemed to modulate ethylene production during on-tree ripening in the same way it was observed during ripening of detached apple fruit (Fernández-Cancelo et al., 2022b), since not only the pattern but the intensity of the ethylene peak was closely linked to the activity of ACO when comparing different cultivars (Figures 1C and 1D).

It is well documented, that ethylene biosynthetic enzymes are encoded by different paralogous genes whose expression depends on the fruit development/ripening stage (Shin et al., 2016). In our study, the strong positive correlation between the expression of *MdACS3* and *MdACO1* with ACS and ACO activities highlights the importance of these genes in triggering ethylene production in the last stages of on-tree apple ripening (Figure S4). Likewise, *MdACS3* transcription preceded the expression of *MdACO1*, suggesting that the slight accumulation of ACC caused by the earlier activation of *MdACS3* may be a prerequisite for the activation of *MdACO1* in 'Royal Gala' and 'Opal®', whereas the absence of expression of *MdACS3* in 'Granny Smith' is likely responsible to maintain ethylene production at basal levels in this particular cultivar (Figures 1, S2B and S2C). Interestingly, the expression of *MdACO1* in 'Royal Gala' and 'Opal®', which is typically found in system 2 (Schaffer et al., 2007), was not accompanied by the expression of the corresponding *MdACS* paralogue associated to system 2, *MdACS1,* but rather of *MdACS3,* which has been previously described as characteristic of system 1 (Tan et al., 2013). Based on these observations, it may be assumed that an intermediate system between system 1 and system 2, involving *MdACS3,* may be occurring in the final stages of 'Royal

Gala' and 'Opal®' on-tree development while the expression of *MdACS1* and the full transition to system 2 occurs exclusively when apple fruit is detached from the tree (Tan et al., 2013).

Ethylene response factors (ERFs) are considered to be involved in the regulation of *MdACS* and *MdACO* genes and in the regulation of the fruit responses to ethylene (T. Li et al., 2016). However, the involvement of ERFs during on-tree apple fruit ripening is still elusive. In our study, the expression of the three studied *MdERFs* showed a low positive correlation with ethylene biosynthetic genes or enzymes (Figure S4). In apple, *MdERF1* is considered a positive regulator of ripening (Wang et al., 2007) yet our data showed a similar evolution and high expression of this gene among the three studied cultivars (Figure S2E), regardless on whether the fruit ripened on-tree ('Opal®' and 'Royal Gala') or not ('Granny Smith') and thereby suggesting that its expression may be regulated by developmental or environmental factors not strictly dependent on the fruit ripening pattern. On the other hand, the low of expression of *MdACS1* (Figure S2A) during on-tree ripening was likely caused by the low expression of its positive regulator *MdERF3* (Figure S2F), as suggested in other studies (T. Li et al., 2016). Whether the low expression levels of *MdERF3* were related to the expression of *MdERF2,* a known inhibitor of *MdERF3* and *MdACS1* (T. Li et al., 2016), its however debatable given the low expression of *MdERF2* observed in our study (Figures S2A, S2F and S2G).

In addition to *MdERFs*, ethylene receptors such as *MdETR1* (Cin et al., 2005) may also be involved in the regulation of the fruit response to ethylene. During on-tree fruit development, the expression of *MdETR1* remained low and only increased with the rise in ethylene production in 'Royal Gala' apples (Figure S2H). However, in 'Opal®' apples, which produced ethylene in smaller amounts compared to 'Royal Gala', and 'Granny Smith' apples, which had low and unchanged ethylene emissions, the expression of

MdETR1 remained practically unaffected (Figure S2H). This result suggests that *MdETR1* expression was dependent on the level of ethylene production in each cultivar, which is consistent with previous studies showing that cultivars with high ethylene emission, such as 'Golden Delicious', presented an enhanced *MdETR1* expression (Li et al., 2010). It is then possible that the differences in *MdETR1* expression levels may have contributed to the observed variations in fruit quality parameters among cultivars at the time of harvest (Table 2). The higher expression of *MdETR1* in 'Royal Gala' was linked to a higher rate of firmness loss, a result consistent with previous studies that showed an acceleration of softening in cultivars with higher expression of *MdETR1* (Wang et al., 2009). The expression of *MdETR1* may facilitate the efficient transmission of the ethylene signal and accelerate some changes associated to fruit ripening, pointing out the key role of ethylene receptors in ripening-related quality changes.

This said, strong evidence from model species such as tomato suggests that not only ethylene but its crosstalk with other hormones may be orchestrating fruit ripening events (Wang and Seymour, 2022). Accordingly, several hormones including ABA and its catabolites, as well as IAA were investigated in parallel to ethylene metabolism and will be discussed in the following sections.

Ethylene is activated by IAA via MdARF5 while ABA may participate in ethylene signal transduction.

Although IAA is considered an inhibitor of ethylene and ripening in tomato (Chirinos et al., 2023), some studies conducted during on-tree ripening on other climacteric fruit, such as peach, suggested that auxins may play a role in triggering ethylene metabolism and ripening (Tatsuki et al., 2013). Indeed, the differential ability to produce ethylene during on-tree ripening among the three studied cultivars seemed to depend on their capacity to

accumulate IAA (Figures 1D and 2A), as it was previously suggested during the ripening of detached apple fruit (Busatto et al., 2021; Fernández-Cancelo et al., 2022b). The high positive correlation between ethylene and *MdARF5* found in our study (Figure S4) indicates that this transcription factor mediates in the crosstalk between IAA and ethylene, possibly by triggering the expression of *MdACS3* by binding to its promoter as observed in previous studies in apples (Yue et al., 2020). Hence, the *MdACS3* expression observed in 'Royal Gala' and 'Opal®' apples would account for their enhanced ACS activity resulting in an accumulation of ACC, which may serve as a signal to trigger ACO activity and ethylene production in the last stages of fruit development (Figure 1). Our data also suggest that once ethylene production was activated, the auxin signal may become unnecessary for fruit ripening, and consequently, ethylene may activate GH3-mediated conjugation mechanisms leading to the observed decline of free IAA levels. Similar observations have been previously made in peach (Yue et al., 2019) and tomato (Sravankumar et al., 2018).

Contrastingly, the inability of 'Granny Smith' apples to produce ethylene seems to be caused by the activation of IAA conjugation pathways leading to inactive auxin conjugates such as IAAsp (Figure 2B), which can be driven towards degradation pathways (Kramer and Ackelsberg, 2015). These conjugation pathways would likely be responsible for maintaining low IAA levels and therefore inhibiting *MdARF5* expression and the activation of ethylene metabolism (Figures 1 and 2). Besides, the high expression of *MdARF2* and *MdARF4* in 'Granny Smith' apples (Figures S3A and S3B) suggests that both transcription factors may also be involved in suppressing IAA accumulation and fruit ripening. Indeed, *MdARF2* and *MdARF4* were negatively correlated with compounds that accumulated at the final stages of development, such as ABA and volatile esters and alcohols (Figure S4). Furthermore, *MdARFs*, and particularly *MdARF4,* may be involved

in the auxin-ABA interaction given the association between its expression pattern and the evolution of ABA levels and its catabolites (Figures 2, 3 and S4). As such, the auxin-ABA interaction has been described in other plant species during development (Emenecker and Strader, 2020) and *MdARF2* has been proposed to be involved in the regulation of ABA signalling in apple (Wang et al., 2022). This said, it should be noted that although our data provide a starting point for further studies on auxin-ABA interaction in apple or other climacteric fruits, further research is needed to fully understand the function of *MdARFs* in the hormonal interplay during apple ripening.

ABA has been also proposed to play an active role in climacteric fruit ripening, even as activator of ethylene metabolism during postharvest ripening of peach fruit (García-Pastor et al., 2021). Likewise, our data suggest that ABA and its catabolites are closely related to ethylene metabolism during apple ripening (Figures 3, S2 and S4). In 'Royal Gala' and 'Opal®' cultivars, ABA, PA, and 7-OH-ABA began to accumulate before ethylene production, indicating a potential participation in the onset of the ethylene burst (Figures 1D, 3B, 3C, and 3D). However, the lack of proportionality between ABA concentration and ethylene production intensity (Figures 1D and 3B), as well as the desynchronization between ethylene production and ABA accumulation in apple fruit under certain postharvest conditions (Fernández-Cancelo et al., 2022b), suggests that ABA or its catabolites may only be indirectly involved in the regulation of ethylene biosynthesis during apple ripening. It is also possible that these hormones are synthesised in response to similar stimuli, as for instance, the auxin peak (Emenecker and Strader, 2020), or act co-ordinately to trigger apple ripening. Indeed, high ethylene production during apple postharvest ripening was unable to trigger ripening-associated changes until ABA levels rise (Fernández-Cancelo et al., 2022b), indicating that ABA may mediate the perception of the ethylene signal during development or ripening as also suggested for

other climacteric fruit (Qiao et al., 2021). In the case of 'Granny' apples, characterized by very low ethylene production (Figure 1D), the function of ABA or its catabolites as ethylene mediators seemed not to be necessary, and their concentrations remained very low during the final stages of ripening (Figure 3B). Unfortunately, the similar evolution of ABA and its catabolites –except DPA and ABA-GE– in the last stages of 'Royal Gala' and 'Opal®' development makes difficult to assign a specific role to each ABA-catabolite in the ripening process and ethylene signalling in these cultivars (Figures 1D and 3). However, since ABA catabolites have low or no biological activity, any hypothetical regulation of ethylene signalling and apple ripening would be likely mediated by ABA (Torres et al., 2018; Weng et al., 2016). On the other hand, the strong increase of ABA-GE in 'Opal®' (Figure 3E), an ABA conjugate product (Burla et al., 2013) and the decrease of ABA in the transition from S5 to S6 (Figure 3B), may indicate an attempt to reduce the ethylene signal leading to a slower ripening of 'Opal®' apple if compared to 'Royal Gala'. Since ABA-GE is accumulated under some stress conditions in other species (Han et al., 2020), it is also possible that the behaviour observed in 'Opal®' apples indicates a lack of adaptation of this cultivar to the orchard agronomical or environmental conditions. This said, the high positive correlation among *MdARF5*, ethylene and ABA metabolism suggest that apple ripening is regulated by a complex crosstalk among IAA, ethylene and ABA. However, further studies are required to clarify the involvement of ABA and its catabolites in the regulation of the ethylene signalling in apple, as well as the possible involvement of auxin in ABA biosynthesis and apple ripening in fruit grown under different environments.

Potential crosstalk among sucrose and hormones plays a minor yet cultivar-dependent role in apple biochemical changes

The hormonal crosstalk appears to be fundamental in regulating fruit ripening, which in climacteric fruit not only involves an increase in ethylene production but also significant biochemical shifts including, among others, changes in the levels of sugars, acids, and VOCs (Brumos, 2021). It has been proposed that some of these biochemical changes could be ripening inducers rather than effects of the ripening process. Indeed, sugars and ROS are considered signalling molecules that can interact with hormones and regulate the metabolic changes associated with fruit ripening (Decros et al., 2019; Durán-Soria et al., 2020). For instance, the crosstalk between sucrose and ABA can promote colour changes in non-climacteric fruit like strawberry (Jia et al., 2016). Similarly, it has been proposed that sucrose and ROS may trigger ethylene production and ripening in climacteric fruits such as tomato, pear and peach (D. Li et al., 2016; Lindo-García et al., 2020; Vall-llaura et al., 2022a). In apples, these interactions are less studied, although it has been observed that fruits tending to have higher levels of sucrose produce more ethylene (Fernández-Cancelo et al., 2021). While ethylene is typically associated with the initiation of biochemical shifts in climacteric fruits (Bapat et al., 2010), the changes observed during on-tree apple ripening reveal varying degrees of dependence on ethylene or any other hormones investigated herein (Figure S2).

As previously described in banana and melon (Pech et al., 2008), our results suggest that sugars and acids (Figure 4) evolved independently of ethylene, ABA, and IAA levels in the three cultivars studied (Figure S4). Indeed, no differences among cultivars were observed in the evolution of fructose, ascorbic acid and dehydroascorbic acid (DHA) suggesting that the accumulation of these compounds was regulated at the specie level or strongly influenced by environmental cues (Fenech et al., 2019; Fernández-Cancelo et

al., 2021; Xu et al., 2022). In contrast, the higher accumulation of glucose in 'Granny Smith' and the lower accumulation levels of malic acid in 'Royal Gala', if compared to the other cultivars, seemed to be regulated at the cultivar level yet not associated to the hormonal dynamics. Only sucrose showed some dependence on ethylene production and especially with ABA levels (Figure S4), since this compound increased slowly during early development stages when ethylene and ABA levels were low and then accelerated its accumulation accompanying the increase of ethylene and ABA (Figures 1E, 3B and 4E). In these lines, sucrose has earlier been proposed to be a key compound triggering ripening in both non-climacteric fruit, favouring the increase of ABA levels (Jia et al., 2013), and in climacteric fruit, favouring the biosynthesis of ethylene (Durán-Soria et al., 2020; Lindo-Garcia et al., 2020; Vall-llaura et al. 2021). Based on our results, a minimum concentration of this sugar might be required to activate the biosynthesis of ABA and ethylene in the later stages of apple development (Figures 1A, 3B and 4C). Additionally, the high correlation between sucrose and the auxin response factor *MdARF5* suggests that a complex signalling network involving the crosstalk among sucrose, IAA, ABA and ethylene may ultimately regulate apple ripening, yet further studies at the molecular level would be needed to fully understand the involvement of sucrose on apple ripening.

Phenolic compounds, such as chlorogenic acid, have also been proposed as regulators of fruit ripening by reducing ethylene biosynthesis in apple and inhibiting to some extent softening (Xi et al., 2016). However, our results do not support such statements when comparing multiple cultivars since 'Royal Gala' apples had higher levels of chlorogenic acid and yet showed higher ethylene production. Like for other biochemical compounds, changes on the pulp phenolic composition seemed to be regulated at the cultivar level and not dependent on the hormonal dynamics (Figures 5 and S4). Indeed, the decrease in phenylpropanoid levels, seems to be more influenced by environmental cues (Fernández-

Cancelo et al., 2022a) than ripening hormones, although it is also possible that phenylpropanoids changes during apple development and ripening are related to the decrease in cytokinins content (not determined herein), which is known to decrease during fruit development (McAtee et al., 2013). A similar decrease in phenylpropanoid levels during the last stages of fruit development and ripening is widely reported in the literature for multiple fruit species (i.e. peach: Vall-llaura, Fernández-Cancelo et al., 2022; apple: Fernández-Cancelo et al., 2022a). Only the volatile phenylpropanoid estragole was strongly correlated with ethylene (Figure S5), suggesting the involvement of ethylene in the regulation of estragole biosynthesis likely through *MdOMT* as reported in previous studies (Yauk et al., 2015). Likewise, the activity of alcohol dehydrogenase (ADH) and alcohol acyltransferase (AAT), which mediate alcohol and ester biosynthesis are known to be promoted by ethylene (Schaffer et al., 2007), explaining the high correlation between ethylene and alcohols, such as 1-butanol and 1-pentanol, and volatile esters, particularly straight-chain acetates, in both 'Royal Gala' and 'Opal®' cultivars (Figure S5). However, once ethylene was activated, the levels of esters and alcohols continued to increase independently of ethylene levels, pointing out that their biosynthesis is likely controlled by substrate availability once ADH and AAT are fully expressed (Ortiz et al., 2011). In turn, the production of some alcohols (1-heptanol, 2-methyl-butanol 2-ethyl hexanol) and esters (ethyl acetate, 2-methylbutyl propanoate) in 'Granny Smith' and in the early stages of 'Royal Gala' and 'Opal®' development (Figure 6E), when ethylene levels were in all cases basal, suggests that their biosynthesis may be controlled by ADH and AAT ethylene-independent isoforms (Souleyre et al., 2014). Although it has been proposed that some esters biosynthesis may be triggered by ABA (Wang et al., 2018), the similar correlation among ethylene, ABA and esters discards the involvement of ABA as exclusive regulator of some esters biosynthesis during on-tree apple ripening (Figure S5),

but sustains the potential cooperation between ethylene and ABA in the activation of ripening related changes such as the biosynthesis of these volatiles. On the other hand, aldehydes were produced by all three cultivars during all stages of on-tree ripening, and their levels evolved independently of ethylene and ABA (Figure S5), indicating that lipoxygenase (LOX) and hydroperoxide lyase (HPL) were active independently of the hormonal dynamics and ripening stage (Echeverría et al., 2004; Schaffer et al., 2007). Similarly, the levels of ketones evolved independently of ethylene and ABA, but IAA was highly correlated with 2-pentanone and 3-penten-2-one (Figure S5). Nonetheless, the high correlation among ketones and IAA observed in this study is likely casual and not a consequence of IAA-related regulation, since exogenous IAA treatments in tomato did not enhance the biosynthesis of ketones (Tobaruela et al., 2021).

Procyanidins as potential sources of resistance to blue mould

The biochemical composition of the fruit is also involved in the defence mechanisms against postharvest pathogens. Therefore, the physicochemical changes associated with apple development and ripening are considered to weaken the preformed defences against fungal infection, thereby increasing the fruit susceptibility to postharvest rots, including *P. expansum*, the main postharvest pathogen in apples (Buron-Moles et al., 2015; Vilanova et al., 2014). Extensive literature suggests that changes at the structural level (cell wall composition) and softening may be the main drivers of enhanced disease susceptibility as the fruit ripens (Nybom et al., 2020). This said, changes at the biochemical level (Balsells-Llauradó et al., 2022; Torregrosa et al., 2020) or even at the hormonal level (Forlani et al., 2019) have also been pointed out as putative modulators of the fruit susceptibility to postharvest moulds. Accordingly, to further investigate the contribution of specific biochemical and molecular apple traits to blue mould

susceptibility, a PLS model was built to correlate the biochemical composition of each cultivar and developmental stage with rot development (Figure 7). The model suggested that, as ripening progressed in all three cultivars, fruit susceptibility to blue mould increased until reaching its maximum at the commercial harvest date of each cultivar, which corresponds to S4 for 'Royal Gala' and S6 for 'Granny Smith' and 'Opal®'. (Figure 7). Although no differences in the rot size among cultivars were observed at the commercial harvest, the higher resistance of 'Granny Smith' and higher susceptibility of 'Opal®' during previous developmental stages suggested that differences in chemical composition and hormone dynamics among cultivars could have, to certain extent, a significant impact on rot development (Figure 7A). Ripening-related hormones such as ABA or the ethylene precursor ACC, as well as transcription factors and receptors involved in the regulation of ethylene metabolism (*MdARF5*, *MdERF1* and *MdETR1)*, were highly correlated with the susceptibility to *P. expansum* because of their involvement in the activation of ripening-associated processes (Figures 7B and 7C). Although it has been described that some *MdERFs* participate in the activation of postharvest pathogen resistance processes (Li et al., 2022), the transcription factors analysed in this study did not appear to participate in any of these resistance mechanisms during on-tree ripening. In addition, the accumulation of sugars such as fructose and sucrose, observed during apple ripening, favoured, to some extent, the development of blue mould likely as they serve as a preferred source of carbon for *P. expansum* (Gong et al., 2022) (Figures 7B and 7C). On the other hand, some hormones involved in the maturation process, such as ABA, which is widely known to activate response mechanisms to biotic stress (Lafuente and González-Candelas, 2022) were not associated to enhanced fruit resistance to *P. expansum*. Likewise, and even though auxins have also been proposed to activate defence processes against *P. expansum* (Zhang et al., 2018), in

this study, IAA and IAAsp did not affect the resistance to *P. expansum* when considering different ripening/developmental stages or cultivars (Figures 7B and 7C).

Antioxidant compounds such as ascorbic acid or polyphenols, in addition to some VOCs, have been proposed to inhibit postharvest fungal growth (Torregrosa et al., 2020; Žebeljan et al., 2019). The PLS model showed that phenolic compounds, especially procyanidins, likely conferred resistance against *P. expansum* (Figures 7B and 7C). Considering that during *P. expansum* infection, reactive oxygen species (ROS) accumulates in the host favouring the deterioration and permeability of cell membranes (Wang et al., 2019), it is reasonable to think that the high antioxidant activity of procyanidins (Chinnici et al., 2004), when compared with the other detected compounds, neutralized more efficiently the degradative action of ROS and the colonization capacity of *P. expansum*. In addition to their antioxidant capacity, and since they share common steps in the metabolic pathway, the contribution of procyanidins to *P. expansum* resistance may also be caused by the greater activation of fruit lignification processes that would favour wound healing and reduce the possibilities of fungal growth (Vilanova et al., 2014).

Volatile compounds may also affect blue mould development in different ways. For instance, *P. expansum* is able to produce VOCs to stimulate the activation of specific metabolic pathways in the host for favouring infection, whereas fruit can also emit VOCs as a defence mechanism against rot development (Kim et al., 2018). In the PLS model, the emission of octanoic acid, 2-methylbutyl propanoate, and β-damascone appears to promote rot growth, which is likely coincidental and due to the decreasing trend of these compounds through ripening of all varieties (Figures 7B and 7C). In contrast, 2-phenylethanol, 4-penten-1-yl acetate, and 6-methyl-5-hepten-2-one appear to promote fruit resistance to *P. expansum* which warrants further investigation on the potential

effectiveness of these compounds to slow down *P. expansum* growth (Figures 7B and 7C). Overall, the results of this study suggest that differences in the chemical composition among apple cultivars, particularly procyanidins, sucrose, and some specific VOCs, may play a role in the susceptibility of the fruit to *P. expansum* decay.

Conclusion

The differences in the ethylene production intensity during on-tree ripening among the three studied cultivars depended on their capacity to accumulate IAA, which seems to be necessary to activate ethylene metabolism in a process mediated by *MdARF5*. In parallel, ABA levels followed the same evolution as ethylene, suggesting that ethylene and ABA may respond to similar stimuli, such as the IAA peak, or that the three hormones may act co-ordinately in the last stages of apple development. In this sense, the inability of 'Granny Smith' apples to produce ethylene and accumulate ABA seems to be caused by the activation of IAA conjugation pathways that may prevent the accumulation of IAA. Interestingly, changes in fructose, ascorbic acid and phenolic compounds seem to occur independently of hormonal dynamics, suggesting that other factors (i.e., environment) may regulate their evolution. That said, the accumulation of sucrose before the trigger of ethylene production, as well as its high correlation with ABA and *MdARF5* further reinforce earlier evidence suggesting that sucrose may mediate apple ripening via a complex crosstalk with IAA, ABA and ethylene.

Regardless of their hormonal dependence, the biochemical changes associated with ripening influenced only to some extent apple susceptibility to rot caused by *P. expansum*. While sucrose and fructose appear to serve as substrates favouring fungal growth, the antioxidant activity of phenolic compounds, particularly procyanidins, seems to increase fruit resistance to rot. Given the importance of fruit biochemical composition not only as

a quality parameter but also in resistance to postharvest rot development, further studies are encouraged to determine which specific signals regulate the fruit biochemical composition and the hormonal dynamics during on-tree ripening, as well as their influence on the general apple postharvest behaviour.

Author's contribution

JGB and PFC conceived and designed the experiments. PFC carried out the experiments. MCA and PFC were responsible for the quantification of hormones and phenylpropanoids. GE, and NT assisted with the statistical analysis and data interpretation. JGB, NT and MCA were responsible for the project resources. PFC and JGB drafted the manuscript and all other authors contributed to improving the final version of the manuscript.

Declaration of competing interest

The authors declare that they have no known competing financial interests or personal relationships that could have appeared to influence the work reported in this paper.

Acknowledgements

This work has been financially supported by the Spanish Agencia Estatal de Investigación (AEI) and European Regional Development Fund (ERDF) through the national project PID2020-117607RR-I00 (ENVIRONAPPLE). This work has been also supported by the CERCA Programme from the 'Generalitat de Catalunya'. Thanks are also given to AEI and ERDF for the predoctoral fellowship awarded to PFC (BES-2017-080741). We are also grateful to Monika Jodkowska, Emma Collings, Neus Lamarca and Núria Vall-llaura for their indispensable and outstanding technical support.

References

Anastasiadi, M., Mohareb, F., Redfern, S.P., Berry, M., Simmonds, M.S.J., Terry, L.A., 2017. Biochemical Profile of Heritage and Modern Apple Cultivars and Application of Machine Learning Methods To Predict Usage, Age, and Harvest Season. J. Agric. Food Chem. 65, 5339–5356. https://doi.org/10.1021/acs.jafc.7b00500

Balsells-Llauradó, M., Echeverría, G., Torres, R., Vall-llaura, N., Teixidó, N., Usall, J., 2022. Emission of volatile organic compounds during nectarine-Monilinia laxa interaction and its relationship with fruit susceptibility to brown rot. Postharvest Biology and Technology 192, 111997. https://doi.org/10.1016/j.postharvbio.2022.111997

Bapat, V.A., Trivedi, P.K., Ghosh, A., Sane, V.A., Ganapathi, T.R., Nath, P., 2010. Ripening of fleshy fruit: Molecular insight and the role of ethylene. Biotechnology Advances 28, 94–107. https://doi.org/10.1016/j.biotechadv.2009.10.002

Brumos, J., 2021. Gene regulation in climacteric fruit ripening. Current Opinion in Plant Biology 63, 102042. https://doi.org/10.1016/j.pbi.2021.102042

Bulens, I., Van de Poel, B., Hertog, M.L., De Proft, M.P., Geeraerd, A.H., Nicolaï, B.M., 2011. Protocol: An updated integrated methodology for analysis of metabolites and enzyme activities of ethylene biosynthesis. Plant Methods 7, 17. https://doi.org/10.1186/1746-4811-7-17

Burla, B., Pfrunder, S., Nagy, R., Francisco, R.M., Lee, Y., Martinoia, E., 2013. Vacuolar Transport of Abscisic Acid Glucosyl Ester Is Mediated by ATP-Binding Cassette and Proton-Antiport Mechanisms in Arabidopsis. Plant Physiol. 163, 1446–1458. https://doi.org/10.1104/pp.113.222547

Buron-Moles, G., Torres, R., Teixidó, N., Usall, J., Vilanova, L., Viñas, I., 2015. Characterisation of H_2O_2 production to study compatible and non-host pathogen interactions in orange and apple fruit at different maturity stages. Postharvest Biology and Technology 99, 27–36. https://doi.org/10.1016/j.postharvbio.2014.07.013

Busatto, N., Tadiello, A., Moretto, M., Farneti, B., Populin, F., Vrhovsek, U., Commisso, M., Sartori, E., Sonego, P., Biasioli, F., Costa, G., Guzzo, F., Fontana, P., Engelen, K., Costa, F., 2021. Ethylene-auxin crosstalk regulates postharvest fruit ripening process in apple. Fruit Research 1, 1–13. https://doi.org/10.48130/FruRes-2021-0013

Chinnici, F., Bendini, A., Gaiani, A., Riponi, C., 2004. Radical Scavenging Activities of Peels and Pulps from cv. Golden Delicious Apples as Related to Their Phenolic Composition. J. Agric. Food Chem. 52, 4684–4689. https://doi.org/10.1021/jf049770a

Chirinos, X., Ying, S., Rodrigues, M.A., Maza, E., Djari, A., Hu, G., Liu, M., Purgatto, E., Fournier, S., Regad, F., Bouzayen, M., Pirrello, J., 2023. Transition to ripening in tomato requires hormone-controlled genetic reprogramming initiated in gel tissue. Plant Physiology 191, 610–625. https://doi.org/10.1093/plphys/kiac464

Cin, V.D., Danesin, M., Boschetti, A., Dorigoni, A., Ramina, A., 2005. Ethylene biosynthesis and perception in apple fruitlet abscission (Malus domestica L. Borck). Journal of Experimental Botany 56, 2995–3005. https://doi.org/10.1093/jxb/eri296

Collings, E., Landahl, S., Jodkowska, M., Nayakoti, S., Chinn, J., Rogers, H., Terry, L.A., Alamar, M.C., 2022. Understanding the mechanisms responsible for postharvest tip breakdown in asparagus: a biochemical approach, in: Acta Horticulturae. Presented at the XV International Asparagus Symposium, Córdoba.

Decros, G., Baldet, P., Beauvoit, B., Stevens, R., Flandin, A., Colombié, S., Gibon, Y., Pétriacq, P., 2019. Get the Balance Right: ROS Homeostasis and Redox Signalling in Fruit. Front. Plant Sci. 10, 1091. https://doi.org/10.3389/fpls.2019.01091

Durán-Soria, S., Pott, D.M., Osorio, S., Vallarino, J.G., 2020. Sugar Signaling During Fruit Ripening. Front. Plant Sci. 11, 564917. https://doi.org/10.3389/fpls.2020.564917

Echeverría, G., Graell, J., López, M.L., Lara, I., 2004. Volatile production, quality and aroma-related enzyme activities during maturation of 'Fuji' apples. Postharvest Biology and Technology 31, 217–227. https://doi.org/10.1016/j.postharvbio.2003.09.003

Emenecker, R.J., Strader, L.C., 2020. Auxin-Abscisic Acid Interactions in Plant Growth and Development. Biomolecules 10, 281. https://doi.org/10.3390/biom10020281

Favre, L., Hunter, D.A., O'Donoghue, E.M., Erridge, Z.A., Napier, N.J., Somerfield, S.D., Hunt, M., McGhie, T.K., Cooney, J.M., Saei, A., Chen, R.K.Y., McKenzie, M.J., Brewster, D., Martin, H., Punter, M., Carr, B., Tattersall, A., Johnston, J.W., Gibon, Y., Heyes, J.A., Lill, R.E., Brummell, D.A., 2022. Integrated multi-omic analysis of fruit maturity identifies biomarkers with drastic abundance shifts spanning the harvest period in 'Royal Gala' apple. Postharvest Biology and Technology 193, 112059. https://doi.org/10.1016/j.postharvbio.2022.112059

Fenech, M., Amaya, I., Valpuesta, V., Botella, M.A., 2019. Vitamin C Content in Fruits: Biosynthesis and Regulation. Front. Plant Sci. 9, 2006. https://doi.org/10.3389/fpls.2018.02006

Fernández-Cancelo, P., Iglesias-Sanchez, A., Torres-Montilla, S., Ribas-Agustí, A., Teixidó, N., Rodriguez-Concepcion, M., Giné-Bordonaba, J., 2022a. Environmentally driven transcriptomic and metabolic changes leading to color differences in "Golden Reinders" apples. Front. Plant Sci. 13, 913433. https://doi.org/10.3389/fpls.2022.913433

Fernández-Cancelo, P., Muñoz, P., Echeverría, G., Larrigaudière, C., Teixidó, N., Munné-Bosch, S., Giné-Bordonaba, J., 2022b. Ethylene and abscisic acid play a key role in modulating apple ripening after harvest and after cold-storage. Postharvest Biology and Technology 188, 111902. https://doi.org/10.1016/j.postharvbio.2022.111902

Fernández-Cancelo, P., Teixidó, N., Echeverría, G., Torres, R., Larrigaudière, C., Giné-Bordonaba, J., 2021. Dissecting the influence of the orchard location and the maturity at harvest on apple quality, physiology and susceptibility to major postharvest pathogens. Scientia Horticulturae 285, 110159. https://doi.org/10.1016/j.scienta.2021.110159

Fernie, A.R., Alseekh, S., 2018. Defining the convergence of ethylene and auxin signaling in tomato. New Phytol 219, 479–481. https://doi.org/10.1111/nph.15251

Forlani, S., Masiero, S., Mizzotti, C., 2019. Fruit ripening: the role of hormones, cell wall modifications, and their relationship with pathogens. Journal of Experimental Botany 70, 2993–3006. https://doi.org/10.1093/jxb/erz112

García-Pastor, M.E., Falagán, N., Giné-Bordonaba, J., Wójcik, D.A., Terry, L.A., Alamar, M.C., 2021. Cultivar and tissue-specific changes of abscisic acid, its catabolites and individual sugars during postharvest handling of flat peaches (Prunus persica cv. platycarpa). Postharvest Biology and Technology 181, 111688. https://doi.org/10.1016/j.postharvbio.2021.111688

Giné-Bordonaba, J., Cantín, C.M., Echeverría, G., Ubach, D., Larrigaudière, C., 2016. The effect of chilling injury-inducing storage conditions on quality and consumer acceptance of different Prunus persica cultivars. Postharvest Biology and Technology 115, 38–47. https://doi.org/10.1016/j.postharvbio.2015.12.006

Giné-Bordonaba, J., Echeverria, G., Duaigües, E., Bobo, G., Larrigaudière, C., 2019. A comprehensive study on the main physiological and biochemical changes occurring during growth and on-tree ripening of two apple varieties with different postharvest behaviour. Plant Physiology and Biochemistry 135, 601–610. https://doi.org/10.1016/j.plaphy.2018.10.035

Gong, D., Bi, Y., Zong, Y., Li, Y., Sionov, E., Prusky, D., 2022. Dynamic Change of Carbon and Nitrogen Sources in Colonized Apples by *Penicillium expansum*. Foods 11, 3367. https://doi.org/10.3390/foods11213367

Han, Y., Watanabe, S., Shimada, H., Sakamoto, A., 2020. Dynamics of the leaf endoplasmic reticulum modulate β-glucosidase-mediated stress-activated ABA production from its glucosyl ester. Journal of Experimental Botany 71, 2058–2071. https://doi.org/10.1093/jxb/erz528

Ji, Y., Wang, A., 2021. Recent Advances in Phytohormone Regulation of Apple-Fruit Ripening. Plants 10, 2061. https://doi.org/10.3390/plants10102061

Jia, H., Jiu, S., Zhang, C., Wang, C., Tariq, P., Liu, Z., Wang, B., Cui, L., Fang, J., 2016. Abscisic acid and sucrose regulate tomato and strawberry fruit ripening through the abscisic acid-stress-ripening transcription factor. Plant Biotechnol J 14, 2045–2065. https://doi.org/10.1111/pbi.12563

Jia, H., Wang, Y., Sun, M., Li, B., Han, Y., Zhao, Y., Li, X., Ding, N., Li, C., Ji, W., Jia, W., 2013. Sucrose functions as a signal involved in the regulation of strawberry fruit development and ripening. New Phytol 198, 453–465. https://doi.org/10.1111/nph.12176

Jiang, Y., Joyce, D.C., Macnish, A.J., 2000. Effect of Abscisic Acid on Banana Fruit Ripening in Relation to the Role of Ethylene. J Plant Growth Regul 19, 106–111. https://doi.org/10.1007/s003440000011

Kim, S.M., Lee, S.M., Seo, J.-A., Kim, Y.-S., 2018. Changes in volatile compounds emitted by fungal pathogen spoilage of apples during decay. Postharvest Biology and Technology 146, 51–59. https://doi.org/10.1016/j.postharvbio.2018.08.003

Kramer, E.M., Ackelsberg, E.M., 2015. Auxin metabolism rates and implications for plant development. Front. Plant Sci. 6. https://doi.org/10.3389/fpls.2015.00150

Kumar, V., Irfan, M., Ghosh, S., Chakraborty, N., Chakraborty, S., Datta, A., 2016. Fruit ripening mutants reveal cell metabolism and redox state during ripening. Protoplasma 253, 581–594. https://doi.org/10.1007/s00709-015-0836-z

Lafuente, M.T., González-Candelas, L., 2022. The Role of ABA in the Interaction between Citrus Fruit and Penicillium digitatum. IJMS 23, 15796. https://doi.org/10.3390/ijms232415796

Li, D., Mou, W., Wang, Y., Li, L., Mao, L., Ying, T., Luo, Z., 2016. Exogenous sucrose treatment accelerates postharvest tomato fruit ripening through the influence on its metabolism and enhancing ethylene biosynthesis and signaling. Acta Physiol Plant 38, 225. https://doi.org/10.1007/s11738-016-2240-5

Li, J., Zhu, H., Yuan, R., 2010. Profiling the Expression of Genes Related to Ethylene Biosynthesis, Ethylene Perception, and Cell Wall Degradation during Fruit Abscission and Fruit Ripening in Apple. J. Amer. Soc. Hort. Sci. 135, 391–401. https://doi.org/10.21273/JASHS.135.5.391

Li, S., Wu, P., Yu, X., Cao, J., Chen, X., Gao, L., Chen, K., Grierson, D., 2022. Contrasting Roles of Ethylene Response Factors in Pathogen Response and Ripening in Fleshy Fruit. Cells 11, 2484. https://doi.org/10.3390/cells11162484

Li, T., Tan, D., Liu, Z., Jiang, Z., Wei, Y., Zhang, L., Li, X., Yuan, H., Wang, A., 2015. Apple *MdACS6* Regulates Ethylene Biosynthesis During Fruit Development Involving Ethylene-Responsive Factor. Plant Cell Physiol 56, 1909–1917. https://doi.org/10.1093/pcp/pcv111

Li, T., Jiang, Z., Zhang, L., Tan, D., Wei, Y., Yuan, H., Li, Tianlai, Wang, A., 2016. Apple (*Malus domestica*) MdERF2 negatively affects ethylene biosynthesis during fruit ripening by suppressing *MdACS1* transcription. Plant J 88, 735–748. https://doi.org/10.1111/tpj.13289

Lindo-García, V., Larrigaudière, C., Echeverría, G., Murayama, H., Soria, Y., Giné-Bordonaba, J., 2019. New insights on the ripening pattern of 'Blanquilla' pears: A comparison between on- and off-tree ripened fruit. Postharvest Biology and Technology 150, 112–121. https://doi.org/10.1016/j.postharvbio.2018.12.013

Lindo-García, V., Muñoz, P., Larrigaudière, C., Munné-Bosch, S., Giné-Bordonaba, J., 2020. Interplay between hormones and assimilates during pear development and ripening and its relationship with the fruit postharvest behaviour. Plant Science 291, 110339. https://doi.org/10.1016/j.plantsci.2019.110339

McAtee, P., Karim, S., Schaffer, R., David, K., 2013. A dynamic interplay between phytohormones is required for fruit development, maturation, and ripening. Front. Plant Sci. 4. https://doi.org/10.3389/fpls.2013.00079

Muller, P.Y., Janovjak, H., Miserez, A.R., Dobbie, Z., 2002. Short technical report processing of gene expression data generated by quantitative real-time RT-PCR. Biotechniques 32, 1372–1379.

Nybom, H., Ahmadi-Afzadi, M., Rumpunen, K., Tahir, I., 2020. Review of the Impact of Apple Fruit Ripening, Texture and Chemical Contents on Genetically Determined Susceptibility to Storage Rots. Plants 9, 831. https://doi.org/10.3390/plants9070831

Ortiz, A., Graell, J., Lara, I., 2011. Volatile ester-synthesising capacity throughout on-tree maturation of 'Golden Reinders' apples. Scientia Horticulturae 131, 6–14. https://doi.org/10.1016/j.scienta.2011.09.020

Pattyn, J., Vaughan-Hirsch, J., Van de Poel, B., 2021. The regulation of ethylene biosynthesis: a complex multilevel control circuitry. New Phytol 229, 770–782. https://doi.org/10.1111/nph.16873

Pech, J.C., Bouzayen, M., Latché, A., 2008. Climacteric fruit ripening: Ethylene-dependent and independent regulation of ripening pathways in melon fruit. Plant Science 175, 114–120. https://doi.org/10.1016/j.plantsci.2008.01.003

Qiao, H., Zhang, H., Wang, Z., Shen, Y., 2021. Fig fruit ripening is regulated by the interaction between ethylene and abscisic acid. J. Integr. Plant Biol. 63, 553–569. https://doi.org/10.1111/jipb.13065

Schaffer, R.J., Friel, E.N., Souleyre, E.J.F., Bolitho, K., Thodey, K., Ledger, S., Bowen, J.H., Ma, J.-H., Nain, B., Cohen, D., Gleave, A.P., Crowhurst, R.N., Janssen, B.J., Yao, J.-L., Newcomb, R.D., 2007. A Genomics Approach Reveals That Aroma Production in Apple Is Controlled by Ethylene Predominantly at the

Final Step in Each Biosynthetic Pathway. Plant Physiology 144, 1899–1912. https://doi.org/10.1104/pp.106.093765

Sfakiotakis, E.M., Dilley, D.R., 1973. Internal Ethylene Concentrations in Apple Fruits Attached to or Detached from the Tree1. J. Amer. Soc. Hort. Sci. 98, 501–503. https://doi.org/10.21273/JASHS.98.5.501

Shin, S., Lee, J., Rudell, D., Evans, K., Zhu, Y., 2016. Transcriptional Regulation of Auxin Metabolism and Ethylene Biosynthesis Activation During Apple (*Malus × domestica*) Fruit Maturation. J Plant Growth Regul 35, 655–666. https://doi.org/10.1007/s00344-015-9568-8

Souleyre, E.J.F., Chagné, D., Chen, X., Tomes, S., Turner, R.M., Wang, M.Y., Maddumage, R., Hunt, M.B., Winz, R.A., Wiedow, C., Hamiaux, C., Gardiner, S.E., Rowan, D.D., Atkinson, R.G., 2014. The *AAT1* locus is critical for the biosynthesis of esters contributing to 'ripe apple' flavour in 'Royal Gala' and 'Granny Smith' apples. Plant J 78, 903–915. https://doi.org/10.1111/tpj.12518

Sravankumar, T., Akash, Naik, N., Kumar, R., 2018. A ripening-induced SlGH3-2 gene regulates fruit ripening via adjusting auxin-ethylene levels in tomato (Solanum lycopersicum L.). Plant Mol Biol 98, 455–469. https://doi.org/10.1007/s11103-018-0790-1

Tan, D., Li, T., Wang, A., 2013. Apple 1-Aminocyclopropane-1-Carboxylic Acid Synthase Genes, MdACS1 and MdACS3a, are Expressed in Different Systems of Ethylene Biosynthesis. Plant Mol Biol Rep 31, 204–209. https://doi.org/10.1007/s11105-012-0490-y

Tatsuki, M., Nakajima, N., Fujii, H., Shimada, T., Nakano, M., Hayashi, K., Hayama, H., Yoshioka, H., Nakamura, Y., 2013. Increased levels of IAA are required for system 2 ethylene synthesis causing fruit softening in peach (Prunus persica L. Batsch). Journal of Experimental Botany 64, 1049–1059. https://doi.org/10.1093/jxb/ers381

Tobaruela, E. de C., Gomes, B.L., Bonato, V.C. de B., Lima, E.S. de, Freschi, L., Purgatto, E., 2021. Ethylene and Auxin: Hormonal Regulation of Volatile Compound Production During Tomato (Solanum lycopersicum L.) Fruit Ripening. Front. Plant Sci. 12, 765897. https://doi.org/10.3389/fpls.2021.765897

Torregrosa, L., Echeverria, G., Illa, J., Torres, R., Giné-Bordonaba, J., 2020. Spatial distribution of flavor components and antioxidants in the flesh of 'Conference' pears and its relationship with postharvest pathogens susceptibility. Postharvest Biology and Technology 159, 111004. https://doi.org/10.1016/j.postharvbio.2019.111004

Torres, N., Goicoechea, N., Zamarreño, A.M., Carmen Antolín, M., 2018. Mycorrhizal symbiosis affects ABA metabolism during berry ripening in Vitis vinifera L. cv. Tempranillo grown under climate change scenarios. Plant Science 274, 383–393. https://doi.org/10.1016/j.plantsci.2018.06.009

Vall-llaura, N., Fernández-Cancelo, P., Nativitas-Lima, I., Echeverria, G., Teixidó, N., Larrigaudière, C., Torres, R., Giné-Bordonaba, J., 2022a. ROS-scavenging-associated transcriptional and biochemical shifts during nectarine fruit development and ripening. Plant Physiology and Biochemistry 171, 38–48. https://doi.org/10.1016/j.plaphy.2021.12.022

Vall-llaura, N., Torres, R., Teixidó, N., Usall, J., Giné-Bordonaba, J., 2022b. Untangling the role of ethylene beyond fruit development and ripening: A physiological and molecular perspective focused on the Monilinia-peach interaction. Scientia Horticulturae 301, 111123. https://doi.org/10.1016/j.scienta.2022.111123

Vendrell, M., Buesa, C., 1989. Relationship between abscisic acid content and ripening of apples. Acta Hortic. 389–396. https://doi.org/10.17660/ActaHortic.1989.258.45

Vilanova, L., Viñas, I., Torres, R., Usall, J., Buron-Moles, G., Teixidó, N., 2014. Increasing maturity reduces wound response and lignification processes against *Penicillium expansum* (pathogen) and *Penicillium digitatum* (non-host pathogen) infection in apples. Postharvest Biology and Technology 88, 54–60. https://doi.org/10.1016/j.postharvbio.2013.09.009

Wang, A., Tan, D., Takahashi, A., Zhong Li, T., Harada, T., 2007. MdERFs, two ethylene-response factors involved in apple fruit ripening. Journal of Experimental Botany 58, 3743–3748. https://doi.org/10.1093/jxb/erm224

Wang, A., Tan, D., Tatsuki, M., Kasai, A., Li, T., Saito, H., Harada, T., 2009. Molecular mechanism of distinct ripening profiles in 'Fuji' apple fruit and its early maturing sports. Postharvest Biology and Technology 52, 38–43. https://doi.org/10.1016/j.postharvbio.2008.09.001

Wang, C., Zhao, Y., Han, P., Yu, J., Hao, Y., Xu, Q., You, C., Hu, D., 2022. Auxin response factor gene MdARF2 is involved in ABA signaling and salt stress response in apple. Journal of Integrative Agriculture 21, 2264–2274. https://doi.org/10.1016/S2095-3119(21)63843-1

Wang, D., Seymour, G.B., 2022. Molecular and biochemical basis of softening in tomato. Mol Horticulture 2, 5. https://doi.org/10.1186/s43897-022-00026-z

Wang, S., Saito, T., Ohkawa, K., Ohara, H., Suktawee, S., Ikeura, H., Kondo, S., 2018. Abscisic acid is involved in aromatic ester biosynthesis related with ethylene in green apples. Journal of Plant Physiology 221, 85–93. https://doi.org/10.1016/j.jplph.2017.12.007

Wang, Y., Ji, D., Chen, T., Li, B., Zhang, Z., Qin, G., Tian, S., 2019. Production, Signaling, and Scavenging Mechanisms of Reactive Oxygen Species in Fruit–Pathogen Interactions. IJMS 20, 2994. https://doi.org/10.3390/ijms20122994

Weng, J.-K., Ye, M., Li, B., Noel, J.P., 2016. Co-evolution of Hormone Metabolism and Signaling Networks Expands Plant Adaptive Plasticity. Cell 166, 881–893. https://doi.org/10.1016/j.cell.2016.06.027

Xi, Y., Cheng, D., Zeng, X., Cao, J., Jiang, W., 2016. Evidences for Chlorogenic Acid — A Major Endogenous Polyphenol Involved in Regulation of Ripening and Senescence of Apple Fruit. PLoS ONE 11, e0146940. https://doi.org/10.1371/journal.pone.0146940

Xu, G., Li, C., Qin, S., Xiao, W., Fu, X., Chen, X., Li, L., Li, D., 2022. Changes in Sucrose and Sorbitol Metabolism Cause Differences in the Intrinsic Quality of Peach Fruits Cultivated in Field and Greenhouse Environments. Agronomy 12, 2877. https://doi.org/10.3390/agronomy12112877

Yang, S., Li, D., Li, S., Yang, H., Zhao, Z., 2022. GC-MS Metabolite and Transcriptome Analyses Reveal the Differences of Volatile Synthesis and Gene Expression Profiling between Two Apple Varieties. International Journal of Molecular Sciences 23, 2939. https://doi.org/10.3390/ijms23062939

Yang, X., Song, J., Campbell-Palmer, L., Fillmore, S., Zhang, Z., 2013. Effect of ethylene and 1-MCP on expression of genes involved in ethylene biosynthesis and perception during ripening of apple fruit. Postharvest Biology and Technology 78, 55–66. https://doi.org/10.1016/j.postharvbio.2012.11.012

Yauk, Y., Chagné, D., Tomes, S., Matich, A.J., Wang, M.Y., Chen, X., Maddumage, R., Hunt, M.B., Rowan, D.D., Atkinson, R.G., 2015. The *MdoOTM1* is required for

biosynthesis of methylated phenylpropenes in ripe apple fruit. Plant J 82, 937–950. https://doi.org/10.1111/tpj.12861

Yue, P., Lu, Q., Liu, Z., Lv, T., Li, X., Bu, H., Liu, W., Xu, Y., Yuan, H., Wang, A., 2020. Auxin-activated MdARF5 induces the expression of ethylene biosynthetic genes to initiate apple fruit ripening. New Phytol 226, 1781–1795. https://doi.org/10.1111/nph.16500

Yue, P., Wang, Y., Bu, H., Li, X., Yuan, H., Wang, A., 2019. Ethylene promotes IAA reduction through PuERFs-activated PuGH3.1 during fruit ripening in pear (Pyrus ussuriensis). Postharvest Biology and Technology 157, 110955. https://doi.org/10.1016/j.postharvbio.2019.110955

Žebeljan, A., Vico, I., Duduk, N., Žiberna, B., Urbanek Krajnc, A., 2019. Dynamic changes in common metabolites and antioxidants during Penicillium expansum-apple fruit interactions. Physiological and Molecular Plant Pathology 106, 166–174. https://doi.org/10.1016/j.pmpp.2019.02.001

Zhang, J., Jiang, L., Sun, C., Jin, L., Lin, M., Huang, Y., Zheng, X., Yu, T., 2018. Indole-3-acetic acid inhibits blue mold rot by inducing resistance in pear fruit wounds. Scientia Horticulturae 231, 227–232. https://doi.org/10.1016/j.scienta.2017.12.046

Zhang, M., Yuan, B., Leng, P., 2009. The role of ABA in triggering ethylene biosynthesis and ripening of tomato fruit. Journal of Experimental Botany 60, 1579–1588. https://doi.org/10.1093/jxb/erp026

List of figures

Figure 1. Ethylene biosynthesis, perception and signalling scheme showing the evolution of ACC synthase activity (A), ACC concentration (B), ACC oxidase activity (C), ethylene production (D) and MACC levels (E) during the development and ripening of 'Royal Gala' (■), 'Opal®' (△) and 'Granny Smith' (●) apples. Each point represents the mean of 4 biological replicates. Error bars represent the LSD values (p=0.05) for the interaction cultivar × sampling point for all cultivars from S1 to S4 (LSD1) and for the interaction cultivar × sampling point for 'Opal®' and 'Granny Smith' from S1 to S6 (LSD2). Dashed lines indicate that some steps in the signalling pathway have been omitted. The corresponding transcript levels of *MdACS1*, *MdACS3*, *MdACO1*, *MdERF1*, *MdERF2*, *MdERF3* and *MdETR1* are represented as heatmaps. Significant differences ($p \leq 0.05$) among cultivars at the same sampling point are denoted by asterisks at the top of the heatmaps, while differences ($p \leq 0.05$) among sampling points at each specific cultivar are indicated by asterisks at the left of the heatmap.

Figure 2. Evolution of indole acetic acid (IAA; A) and indole-3-acetyl aspartic acid (IAAsp; B) levels during the development and ripening of 'Royal Gala' (■), 'Opal®' (△) and 'Granny Smith' (●) apples. Each point represents the mean of 4 biological replicates. Error bars represent the LSD values (p=0.05) for the interaction cultivar × sampling point for all cultivars from S1 to S4 (LSD1) and for the interaction cultivar × sampling point for 'Opal®' and 'Granny Smith' from S1 to S6 (LSD2). The corresponding transcript levels corresponding to de auxin response factors *MdARF2*, *MdARF4* and *MdARF5* are represented as heatmaps. Significant differences ($p \leq 0.05$) among cultivars at the same sampling point are denoted by asterisks at the top of the heatmaps, while differences ($p \leq 0.05$) among sampling points at each specific cultivar are indicated by asterisks at the left of the heatmap.

Figure 3. Evolution of Neophaseic acid (neoPA, A), abscisic acid (ABA, B), phaseic acid (PA, C), 7'-hydroxy ABA (7'-OH ABA, D), ABA glucose ester (ABA-GE, E), Dihydrophaseic acid (DPA, F) during the development and ripening of 'Royal Gala' (■), 'Opal®' (△) and 'Granny Smith' (●) apples. Dashed lines indicate that some steps in the metabolic pathway have been omitted. Each point represents the mean of 4 biological replicates. Error bars represent the LSD values (p=0.05) for the interaction cultivar × sampling point for all cultivars from S1 to S4 (LSD1) and for the interaction cultivar × sampling point for 'Opal®' and 'Granny Smith' from S1 to S6 (LSD2).

Figure 4. Evolution of glucose (A), fructose (C), sucrose (E), malic acid (B), ascorbic acid (D) and dehydroascorbic acid (DHA, F) during the development of 'Royal Gala' (■), 'Opal®' (△) and 'Granny Smith' (●) apples. Each point represents the mean of 4 biological replicates. Error bars represent the LSD values (p=0.05) for the interaction cultivar × sampling point for all cultivars from S1 to S4 (LSD1) and for the interaction cultivar × sampling point for 'Opal®' and 'Granny Smith' from S1 to S6 (LSD2).

Figure 5. Comparison of phenolic compounds metabolism in 'Royal Gala' (■), 'Opal®' (△) and 'Granny Smith' (●) during fruit development. Dashed lines indicate that some steps in the metabolic pathway have been omitted. Each point represents the mean of 4 biological replicates. Error bars represent the LSD values (p=0.05) for the interaction cultivar × sampling point for all cultivars from S1 to S4 (LSD1) and for the interaction cultivar × sampling point for 'Opal®' and 'Granny Smith' from S1 to S6 (LSD2).

Figure 6. Evolution of total volatile alcohols (A), total volatile aldehydes (B), total volatile esters (C) and total volatile phenylpropanoids during the development of 'Royal Gala' (■), 'Opal®' (△) and 'Granny Smith' (●) apples. Each point represents the mean of 4 biological replicates. Error bars represent the LSD values (p=0.05) for the interaction cultivar × sampling point for all cultivars from S1 to S4 (LSD1) and for the interaction

cultivar × sampling point for 'Opal®' and 'Granny Smith' from S1 to S6 (LSD2). A two-way hierarchical cluster analysis (E) was performed with the average value of each individual VOC detected at each sampling point and cultivar. Colours indicate the amount of each VOC, where green represents low levels and red high levels. Detailed data is available in Supplementary Table S2.

Figure 7. Susceptibility to *P. expansum,* measured as rot diameter 10 days after inoculation (A), of 'Royal Gala' (RG, red), 'Opal®' (OP, yellow) and 'Granny Smith' (GS, green) apples at each sampling point (A). Each bar represents the mean of 20 biological replicates. Letters, whenever available, indicate significant differences among cultivars at each sampling point according to Tukey test ($p \leq 0.05$). The contribution of each metabolite to *P. expansum* growth was analysed using a Partial Least Squares (PLS) regression model. The correlation loading plots (B) obtained from the Partial Least Squares (PLS) regression model was used to analyse the *P. expansum* growth for each cultivar and sampling point and the contribution of each metabolite and gene to the apple susceptibility to *P. expansum*. The importance of each variable in the model is detailed in the variable importance plot (VIP) which includes the regression coefficients for each variable (C). The code used to denotate each VOC is presented in Supplementary Table S2.

List of Supplementary Figures

Supplementary Figure S1. Evolution of fruit diameter during the development of 'Royal Gala' (■), 'Opal®' (△) and 'Granny Smith' (●) apples. Each point represents the mean of 20 biological replicates. Error bars represent the LSD values (p=0.05) for the interaction cultivar × sampling point for all cultivars from S1 to S4 (LSD1) and for the interaction cultivar × sampling point for 'Opal®' and 'Granny Smith' from S1 to S6 (LSD2).

Supplementary Figure S2. Expression profile of ethylene biosynthetic genes (A, B, C), ethylene response factors (*MdERFs*; D, E, F) and ethylene receptor *MdETR1* (G) studied during the development of 'Royal Gala' (■), 'Opal®' (△) and 'Granny Smith' (●) apples. Each point represents the mean of 4 biological replicates. Error bars represent the LSD values (p=0.05) for the interaction cultivar × sampling point for all cultivars from S1 to S4 (LSD1) and for the interaction cultivar × sampling point for 'Opal®' and 'Granny Smith' from S1 to S6 (LSD2).

Supplementary Figure S3. Expression profile of auxin response factors *MdARF2* (A), *MdARF4* (B) and *MdARF5* (C) studied during the development of 'Royal Gala' (■), 'Opal®' (△) and 'Granny Smith' (●) apples. Error bars represent the LSD values (p=0.05) for the interaction cultivar × sampling point for all cultivars from S1 to S4 (LSD1) and for the interaction cultivar × sampling point for 'Opal®' and 'Granny Smith' from S1 to S6 (LSD2).

Supplementary Figure S4. Correlations among the different parameters (metabolites, enzymatic activities, and gene expression) studied during the development of 'Royal Gala', 'Opal®' and 'Granny Smith' apples. The size of the circle for each correlation and the colour depict the significance and the correlation coefficient, respectively. Positive correlation coefficients are displayed in blue and negative correlation coefficients in red.

Supplementary Figure S5. Correlations among the individual volatile organic compounds (VOCs) and hormones studied during the development of 'Royal Gala', 'Opal®' and 'Granny Smith' apples. The size of the circle for each correlation and the colour depict the significance and the correlation coefficient, respectively. Positive correlation coefficients are displayed in blue and negative correlation coefficients in red. The code used to denotate each VOC is presented in Supplementary Table S2.

Figure 1.

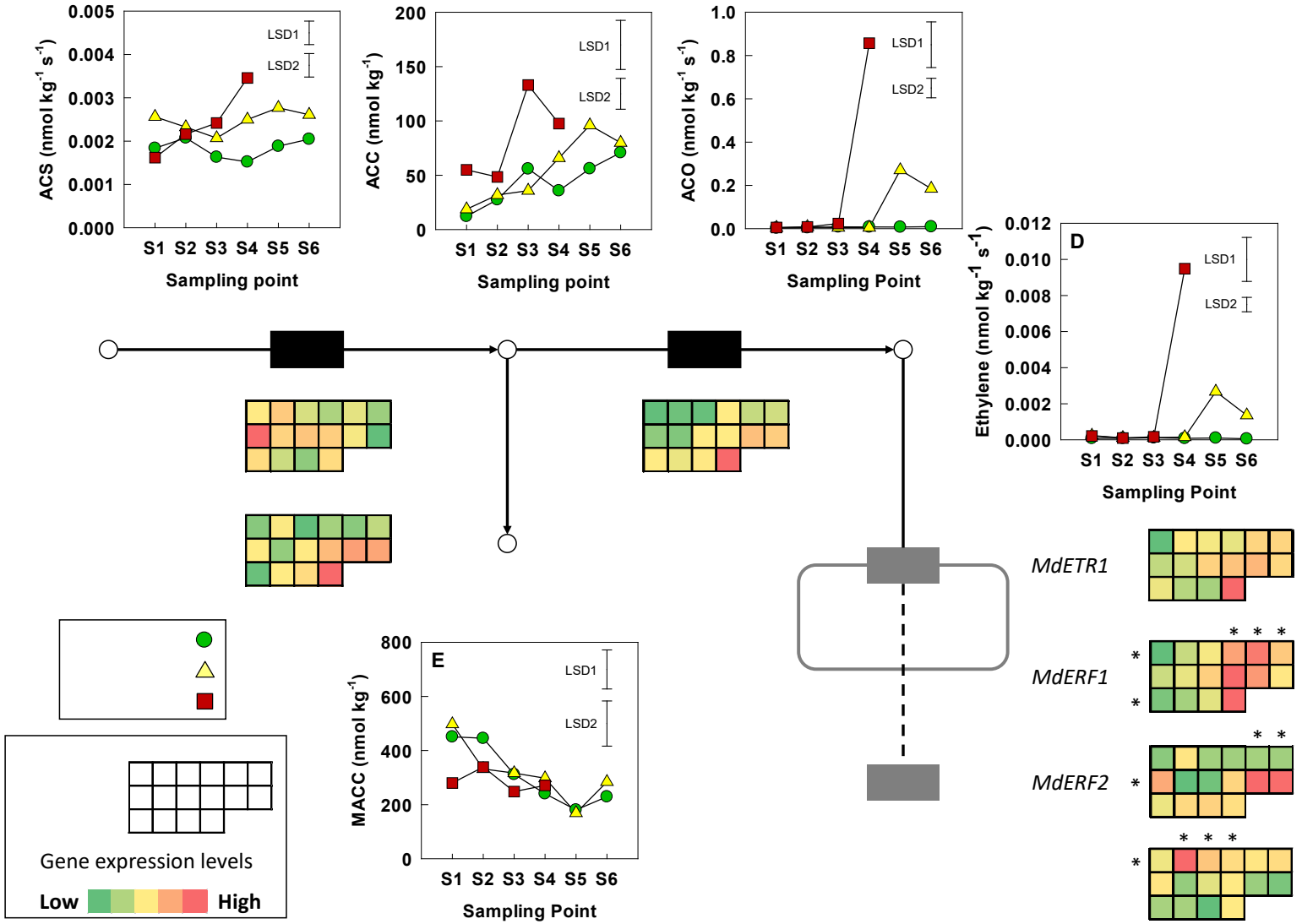
ACS (nmol kg-1 s-1)
0.005
0.004
0.003
0.002
0.001
0.000
LSD1
LSD2
S1 S2 S3 S4 S5 S6
Sampling point
ACC (nmol kg-1)
200
150
100
50
0
LSD1
LSD2
S1 S2 S3 S4 S5 S6
Sampling point
ACO (nmol kg-1 s-1)
1.0
0.8
0.6
0.4
0.2
0.0
LSD1
LSD2
S1 S2 S3 S4 S5 S6
Sampling Point
D
Ethylene (nmol kg-1 s-1)
0.012
0.010
0.008
0.006
0.004
0.002
0.000
LSD1
LSD2
S1 S2 S3 S4 S5 S6
Sampling Point
MdETR1
MdERF1
MdERF2
E
MACC (nmol kg-1)
800
600
400
200
0
LSD1
LSD2
S1 S2 S3 S4 S5 S6
Sampling Point
Gene expression levels
Low
High

Figure 2.

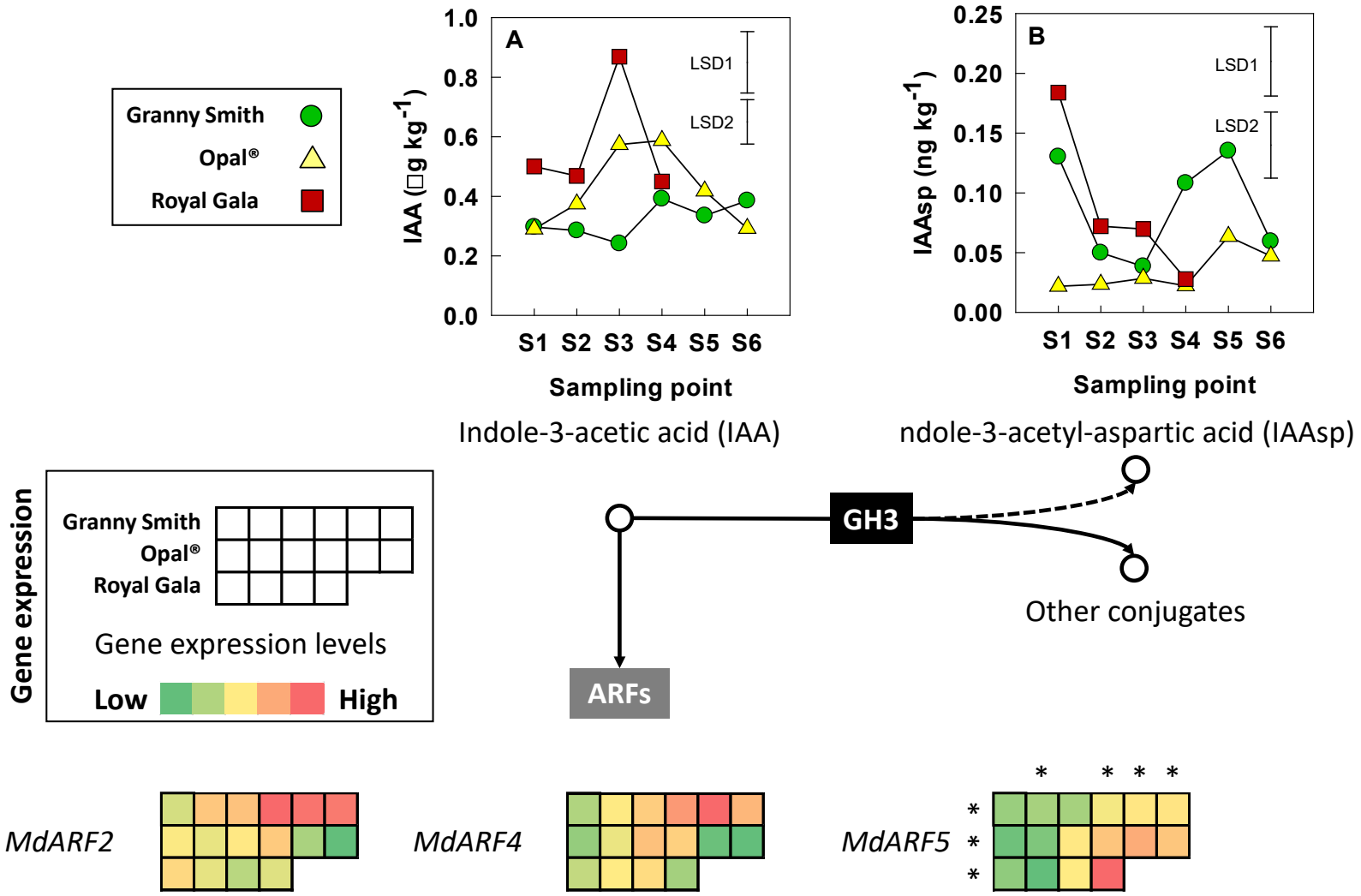
Granny Smith
Opal®
Royal Gala
A
IAA (□g kg-1)
1.0
0.8
0.6
0.4
0.2
0.0
LSD1
LSD2
S1 S2 S3 S4 S5 S6
Sampling point
Indole-3-acetic acid (IAA)
B
IAAsp (ng kg-1)
0.25
0.20
0.15
0.10
0.05
0.00
LSD1
LSD2
S1 S2 S3 S4 S5 S6
Sampling point
ndole-3-acetyl-aspartic acid (IAAsp)
Gene expression
Granny Smith
Opal®
Royal Gala
Gene expression levels
Low
High
GH3
ARFs
Other conjugates
MdARF2
MdARF4
MdARF5
* * * *
* * *

Figure 3.

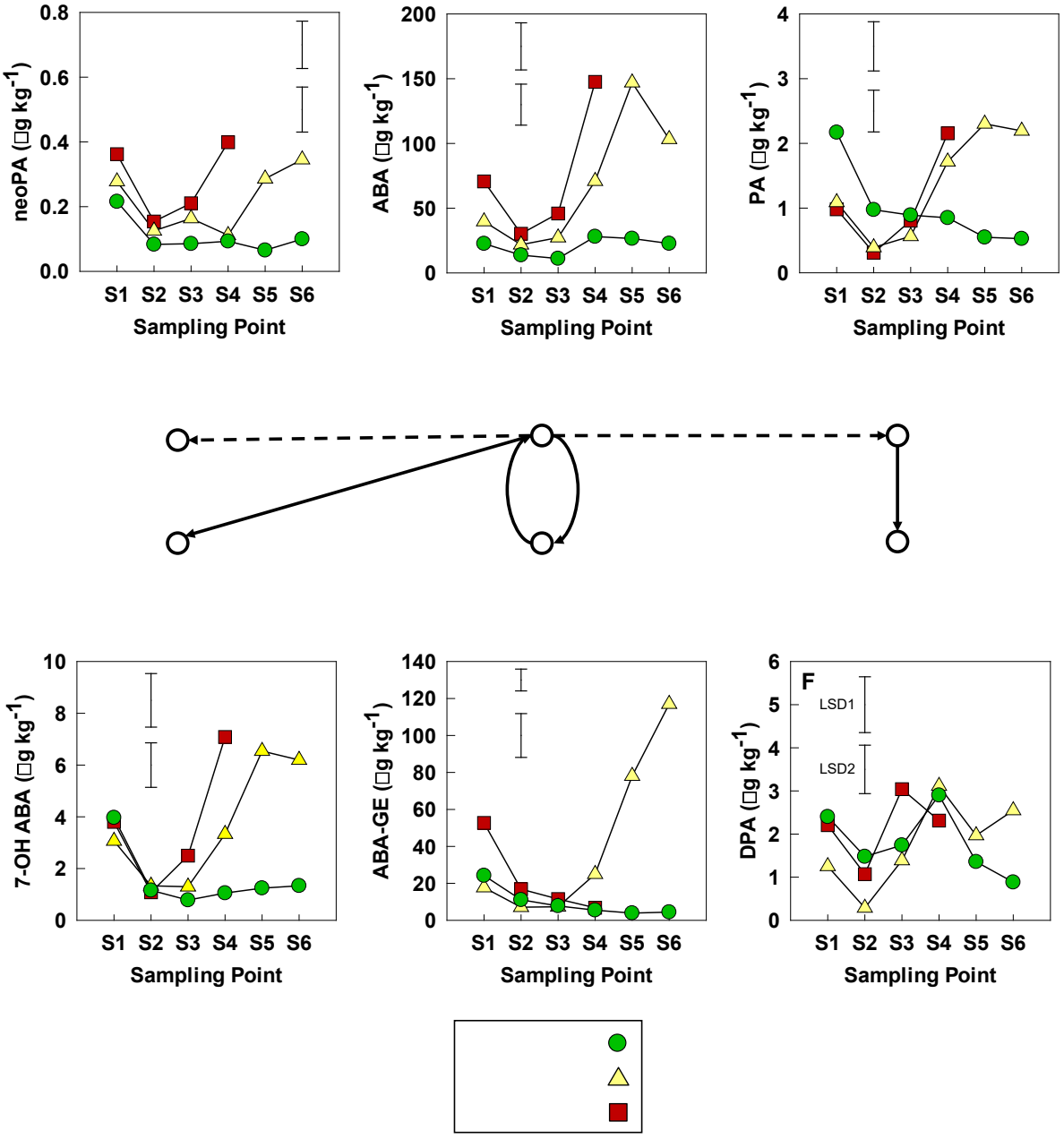
neoPA (□g kg-1)
ABA (□g kg-1)
PA (□g kg-1)
7-OH ABA (□g kg-1)
ABA-GE (□g kg-1)
DPA (□g kg-1)
F
LSD1
LSD2
S1 S2 S3 S4 S5 S6
Sampling Point

Figure 4.

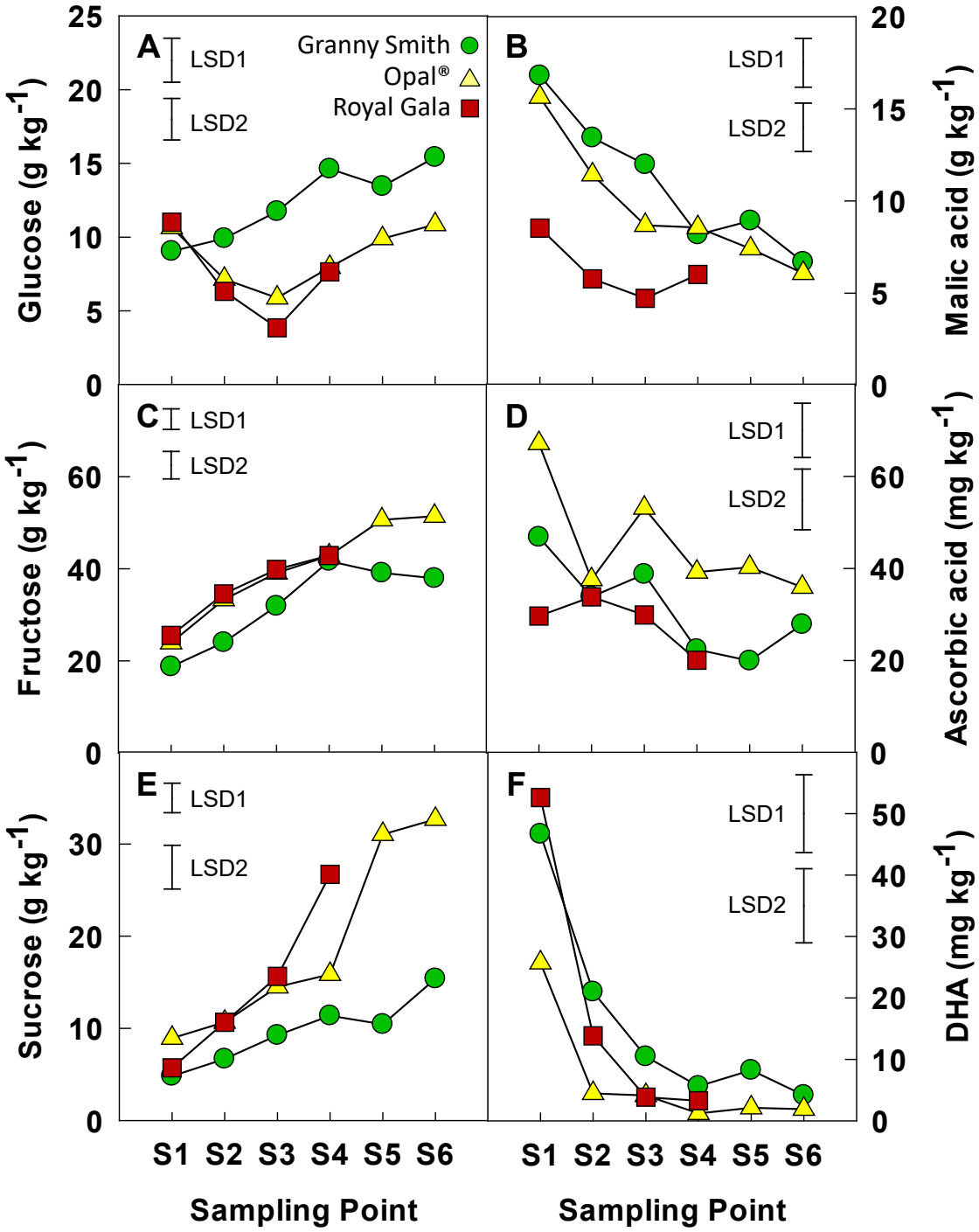
A
B
C
D
E
F
LSD1
LSD2
Granny Smith
Opal®
Royal Gala
Glucose (g kg-1)
Malic acid (g kg-1)
Fructose (g kg-1)
Ascorbic acid (mg kg-1)
Sucrose (g kg-1)
DHA (mg kg-1)
S1 S2 S3 S4 S5 S6
Sampling Point

Figure 5.

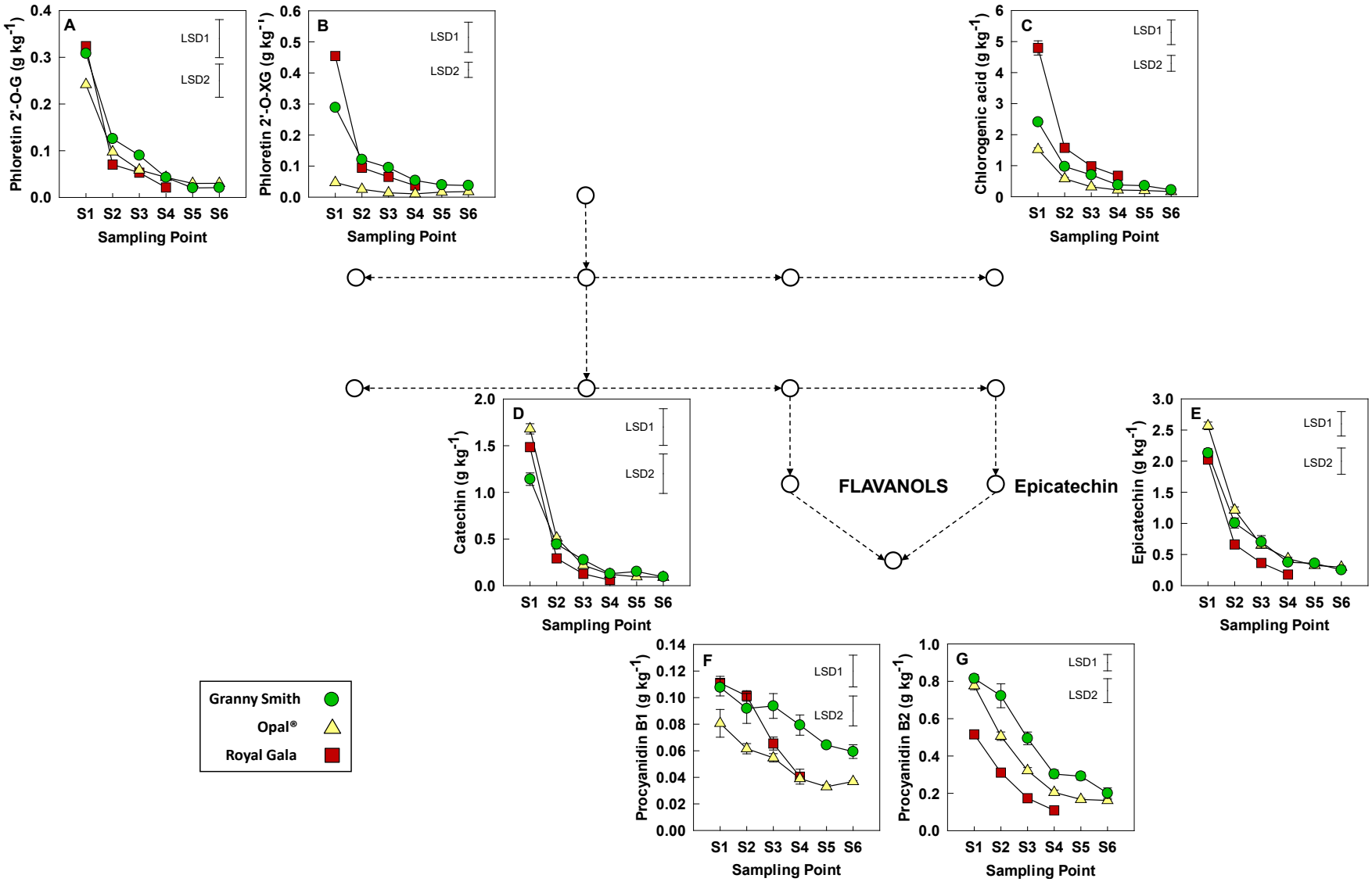
A
Phloretin 2'-O-G (g kg-1)
0.0 0.1 0.2 0.3 0.4
LSD1
LSD2
S1 S2 S3 S4 S5 S6
Sampling Point
B
Phloretin 2'-O-XG (g kg-1)
0.0 0.1 0.2 0.3 0.4 0.5 0.6
LSD1
LSD2
S1 S2 S3 S4 S5 S6
Sampling Point
C
Chlorogenic acid (g kg-1)
0 1 2 3 4 5 6
LSD1
LSD2
S1 S2 S3 S4 S5 S6
Sampling Point
FLAVANOLS
D
Catechin (g kg-1)
0.0 0.5 1.0 1.5 2.0
LSD1
LSD2
S1 S2 S3 S4 S5 S6
Sampling Point
Epicatechin
E
Epicatechin (g kg-1)
0.0 0.5 1.0 1.5 2.0 2.5 3.0
LSD1
LSD2
S1 S2 S3 S4 S5 S6
Sampling Point
F
Procyanidin B1 (g kg-1)
0.00 0.02 0.04 0.06 0.08 0.10 0.12 0.14
LSD1
LSD2
S1 S2 S3 S4 S5 S6
Sampling Point
G
Procyanidin B2 (g kg-1)
0.0 0.2 0.4 0.6 0.8 1.0
LSD1
LSD2
S1 S2 S3 S4 S5 S6
Sampling Point
Granny Smith
Opal®
Royal Gala

Figure 6.

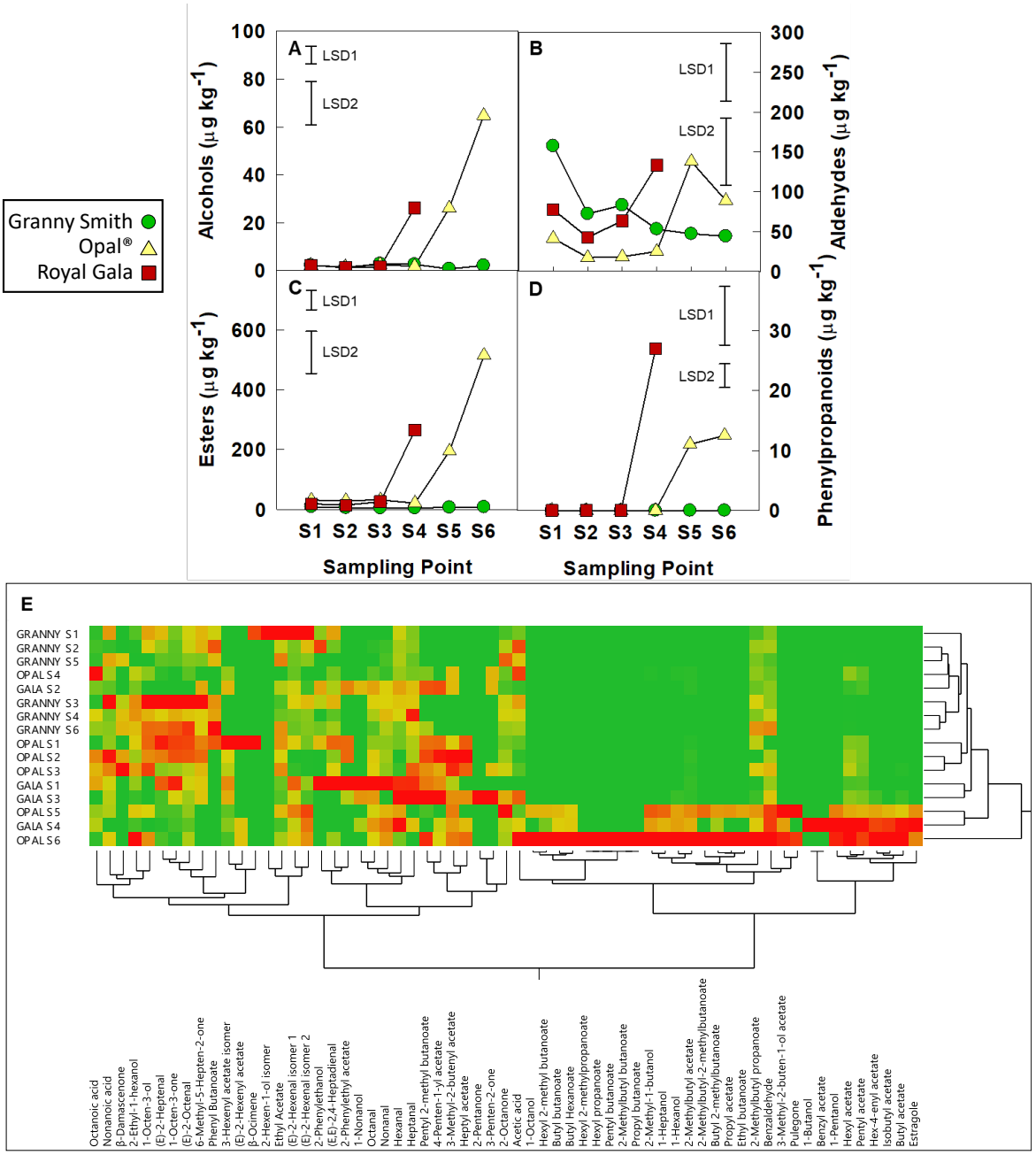
Granny Smith
Opal®
Royal Gala
A
B
C
D
E
LSD1
LSD2
Alcohols (µg kg-1)
Aldehydes (µg kg-1)
Esters (µg kg-1)
Phenylpropanoids (µg kg-1)
S1 S2 S3 S4 S5 S6
Sampling Point
GRANNY S1
GRANNY S2
GRANNY S5
OPAL S4
GALA S2
GRANNY S3
GRANNY S4
GRANNY S6
OPAL S1
OPAL S2
OPAL S3
GALA S1
GALA S3
OPAL S5
GALA S4
OPAL S6
Octanoic acid
Nonanoic acid
β-Damascenone
2-Ethyl-1-hexanol
1-Octen-3-ol
(E)-2-Heptenal
1-Octen-3-one
(E)-2-Octenal
6-Methyl-5-Hepten-2-one
Phenyl Butanoate
3-Hexenyl acetate isomer
(E)-2-Hexenyl acetate
β-Ocimene
2-Hexen-1-ol isomer
Ethyl Acetate
(E)-2-Hexenal isomer 1
(E)-2-Hexenal isomer 2
2-Phenylethanol
(E,E)-2,4-Heptadienal
2-Phenylethyl acetate
1-Nonanol
Octanal
Nonanal
Hexanal
Heptanal
Pentyl 2-methyl butanoate
4-Penten-1-yl acetate
3-Methyl-2-butenyl acetate
Heptyl acetate
2-Pentanone
3-Penten-2-one
2-Octanone
Acetic acid
1-Octanol
Hexyl 2-methyl butanoate
Butyl butanoate
Butyl Hexanoate
Hexyl 2-methylpropanoate
Hexyl propanoate
Pentyl butanoate
2-Methylbutyl butanoate
Propyl butanoate
2-Methyl-1-butanol
1-Heptanol
1-Hexanol
2-Methylbutyl acetate
2-Methylbutyl-2-methylbutanoate
Butyl 2-methylbutanoate
Propyl acetate
Ethyl butanoate
2-Methylbutyl propanoate
Benzaldehyde
3-Methyl-2-buten-1-ol acetate
Pulegone
1-Butanol
Benzyl acetate
1-Pentanol
Hexyl acetate
Pentyl acetate
Hex-4-enyl acetate
Isobutyl acetate
Butyl acetate
Estragole

Figure 7.

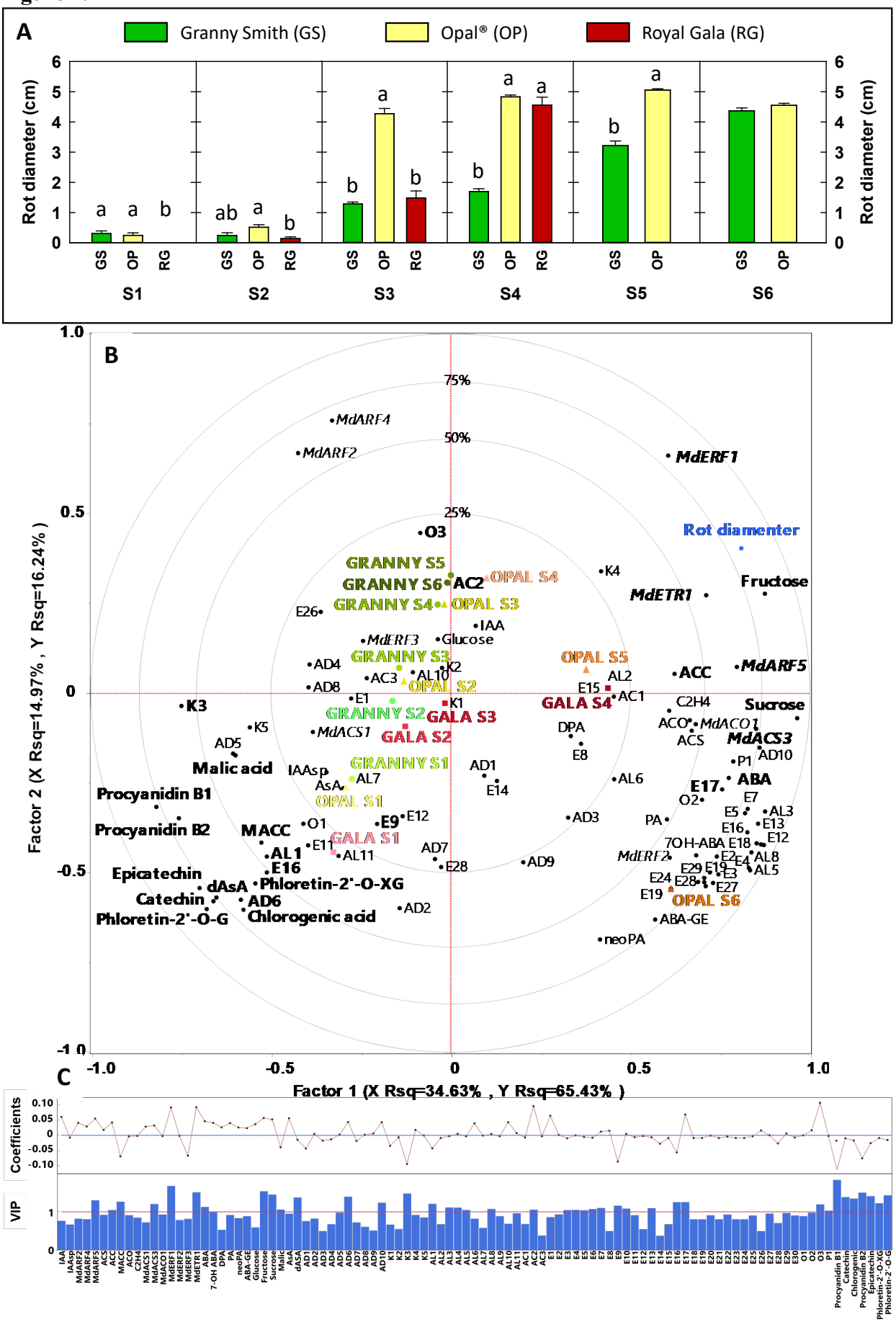
A
Granny Smith (GS)
Opal® (OP)
Royal Gala (RG)
Rot diameter (cm)
S1
S2
S3
S4
S5
S6
B
Factor 2 (X Rsq=14.97% , Y Rsq=16.24%)
Factor 1 (X Rsq=34.63% , Y Rsq=65.43%)
MdARF4
MdARF2
MdERF1
Rot diamenter
O3
GRANNY S5
GRANNY S6
AC2
OPAL S4
K4
Fructose
MdETR1
GRANNY S4
OPAL S3
E26
IAA
MdERF3
Glucose
GRANNY S3
OPAL S5
AD4
K2
AL10
AC3
AL2
ACC
MdARF5
AD8
OPAL S2
E15
E1
K1
AC1
C2H4
K3
GRANNY S2
GALA S3
GALA S4
Sucrose
K5
MdACS1
GALA S2
DPA
ACO
MdACO1
AD5
ACS
MdACS3
E8
P1
AD10
Malic acid
IAAsp
GRANNY S1
AD1
AL7
AL6
E17
ABA
AsA
E14
O2
E7
Procyanidin B1
OPAL S1
AD3
E5
AL3
O1
E9
E12
PA
E16
E13
Procyanidin B2
MACC
GALA S1
7OH-ABA
E18
E12
E11
AD7
MdERF2
E2
AL8
AL1
AL11
E29
E19
E4
AL5
E16
E28
AD9
E24
E3
Epicatechin
dAsA
Phloretin-2'-O-XG
E27
E19
OPAL S6
Catechin
AD6
AD2
ABA-GE
Phloretin-2'-O-G
Chlorogenic acid
neoPA
C
Coefficients
VIP

Figure S1.

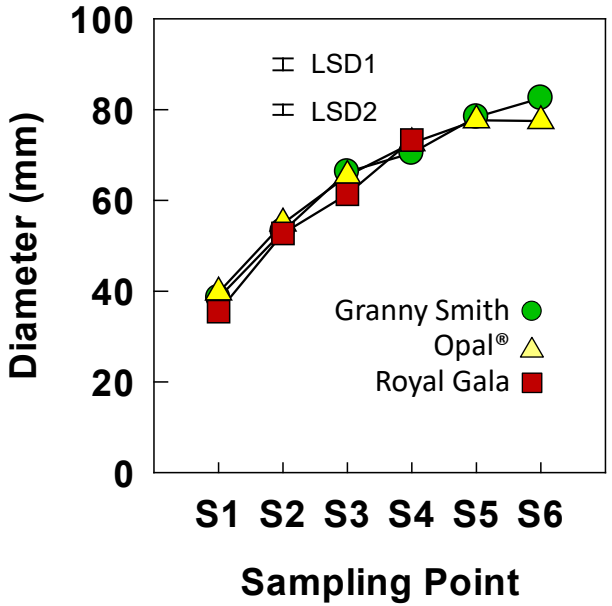
100
80
60
40
20
0
Diameter (mm)
LSD1
LSD2
Granny Smith
Opal®
Royal Gala
S1 S2 S3 S4 S5 S6
Sampling Point

Figure S2.

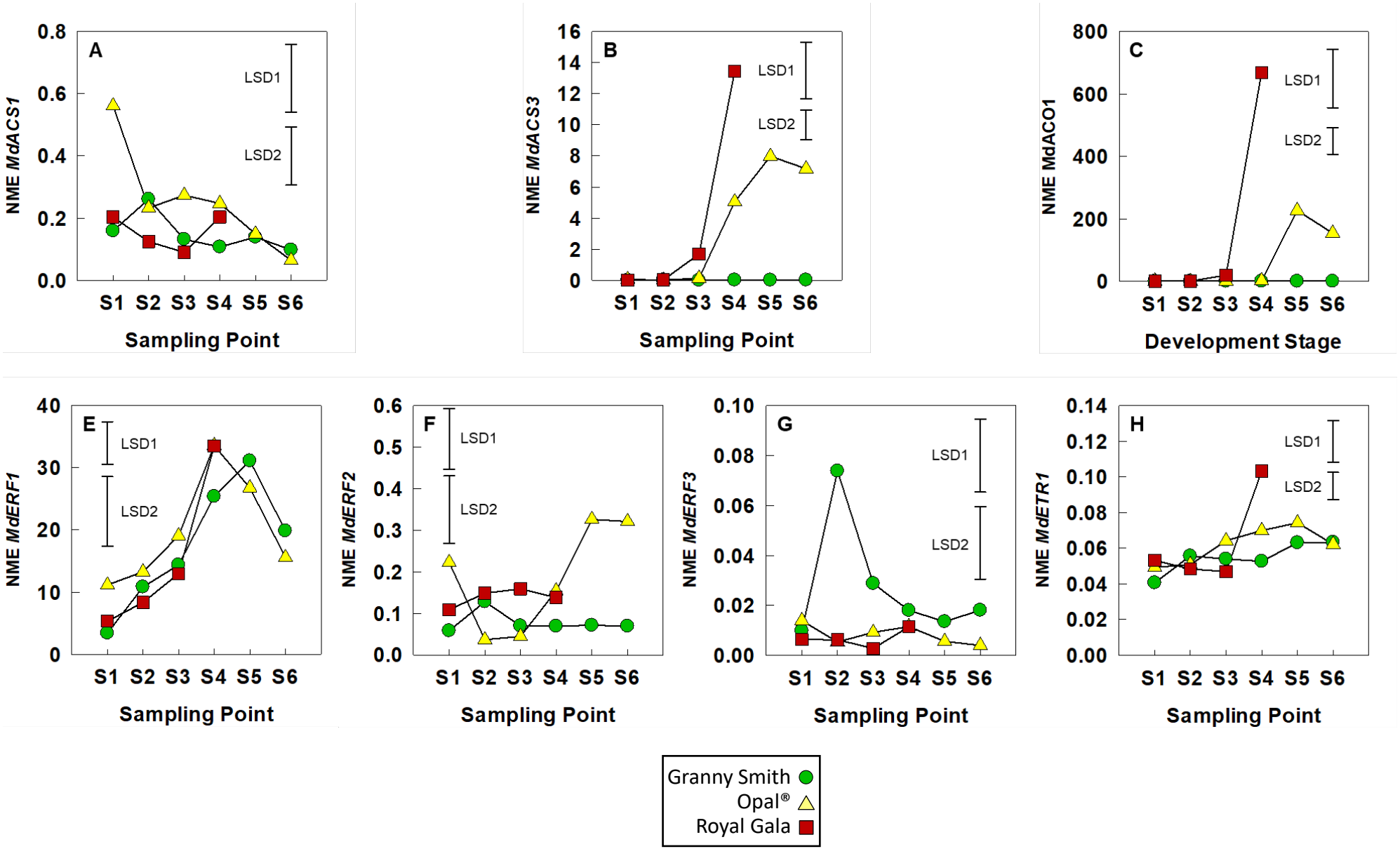
A
NME MdACS1
0.8
0.6
0.4
0.2
0.0
LSD1
LSD2
S1 S2 S3 S4 S5 S6
Sampling Point
B
NME MdACS3
16
14
12
10
8
6
4
2
0
LSD1
LSD2
S1 S2 S3 S4 S5 S6
Sampling Point
C
NME MdACO1
800
600
400
200
0
LSD1
LSD2
S1 S2 S3 S4 S5 S6
Development Stage
E
NME MdERF1
40
30
20
10
0
LSD1
LSD2
S1 S2 S3 S4 S5 S6
Sampling Point
F
NME MdERF2
0.6
0.5
0.4
0.3
0.2
0.1
0.0
LSD1
LSD2
S1 S2 S3 S4 S5 S6
Sampling Point
G
NME MdERF3
0.10
0.08
0.06
0.04
0.02
0.00
LSD1
LSD2
S1 S2 S3 S4 S5 S6
Sampling Point
H
NME MdETR1
0.14
0.12
0.10
0.08
0.06
0.04
0.02
0.00
LSD1
LSD2
S1 S2 S3 S4 S5 S6
Sampling Point
Granny Smith
Opal®
Royal Gala

Figure S3.

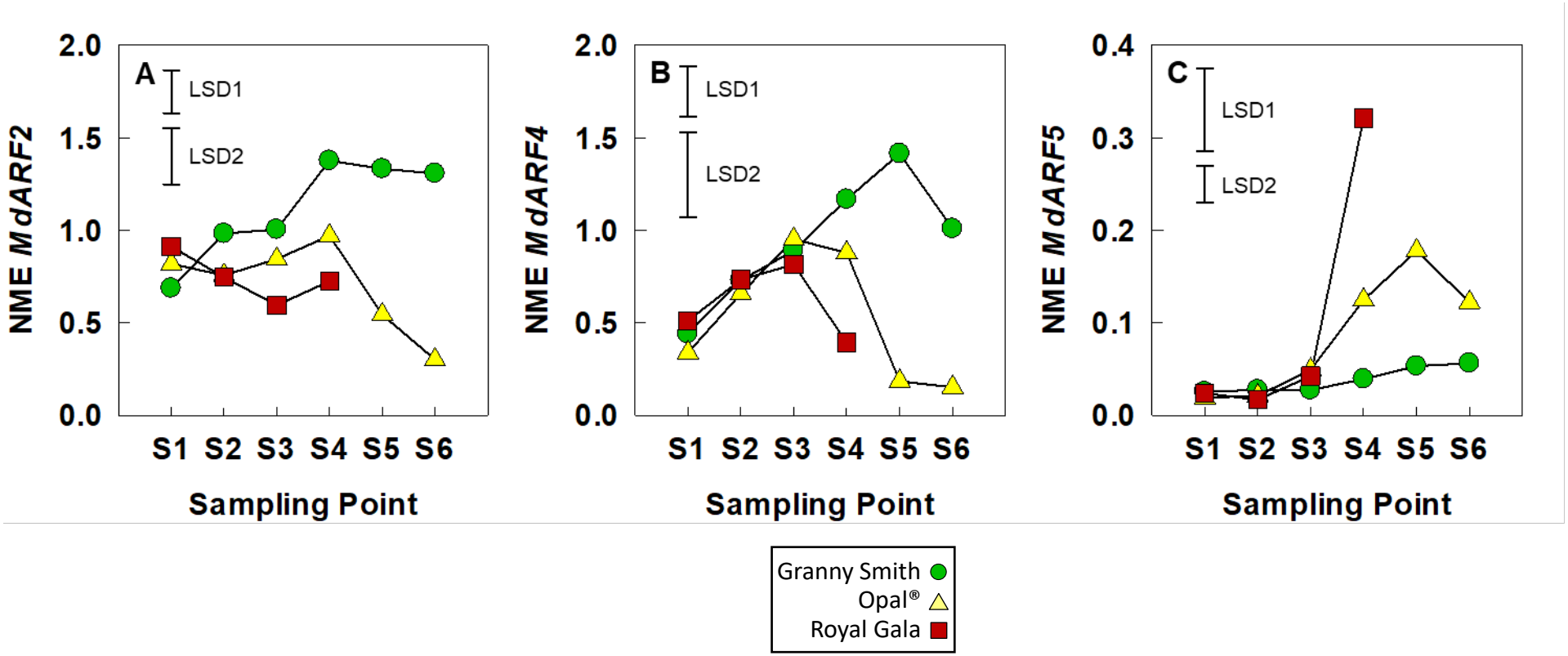
A
B
C
LSD1
LSD2
NME MdARF2
NME MdARF4
NME MdARF5
2.0
1.5
1.0
0.5
0.0
0.4
0.3
0.2
0.1
S1 S2 S3 S4 S5 S6
Sampling Point
Granny Smith
Opal®
Royal Gala

Figure S4.

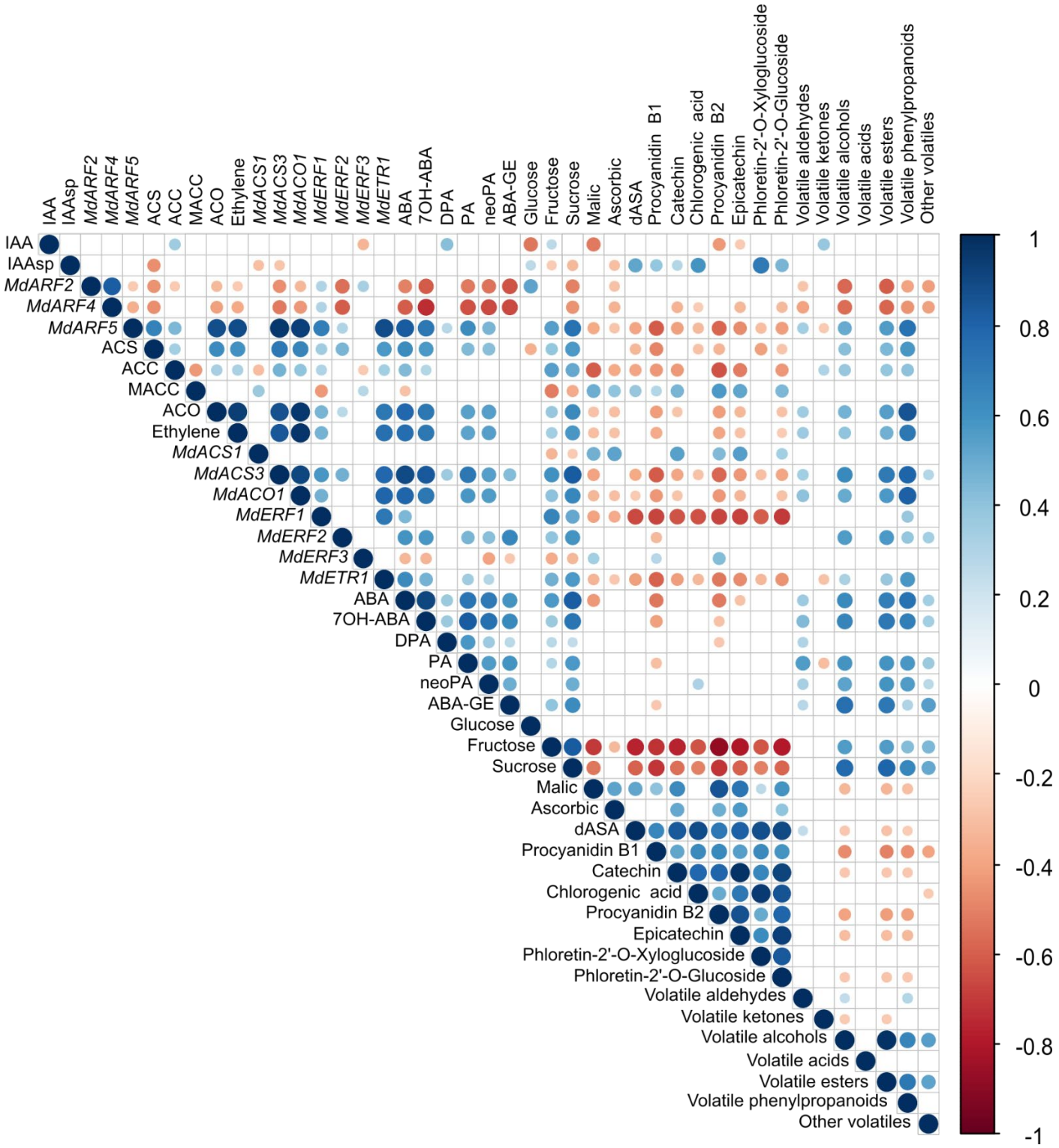
IAA
IAAsp
MdARF2
MdARF4
MdARF5
ACS
ACC
MACC
ACO
Ethylene
MdACS1
MdACS3
MdACO1
MdERF1
MdERF2
MdERF3
MdETR1
ABA
7OH-ABA
DPA
PA
neoPA
ABA-GE
Glucose
Fructose
Sucrose
Malic
Ascorbic
dASA
Procyanidin B1
Catechin
Chlorogenic acid
Procyanidin B2
Epicatechin
Phloretin-2'-O-Xyloglucoside
Phloretin-2'-O-Glucoside
Volatile aldehydes
Volatile ketones
Volatile alcohols
Volatile acids
Volatile esters
Volatile phenylpropanoids
Other volatiles
1
0.8
0.6
0.4
0.2
0
-0.2
-0.4
-0.6
-0.8
-1

Figure S5.

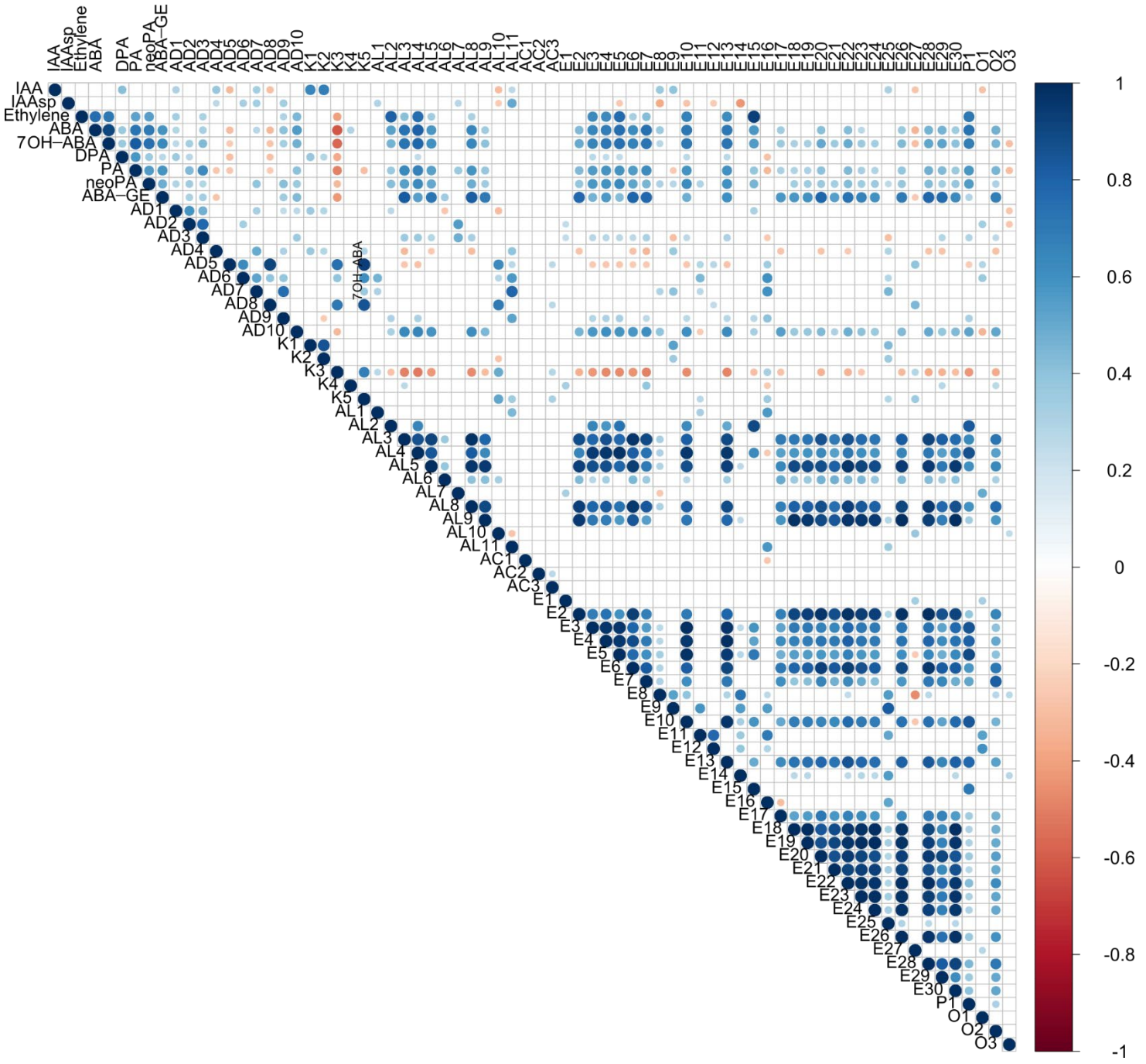
IAA
IAAsp
Ethylene
ABA
7OH–ABA
DPA
PA
neoPA
ABA–GE
AD1
AD2
AD3
AD4
AD5
AD6
AD7
AD8
AD9
AD10
K1
K2
K3
K4
K5
AL1
AL2
AL3
AL4
AL5
AL6
AL7
AL8
AL9
AL10
AL11
AC1
AC2
AC3
E1
E2
E3
E4
E5
E6
E7
E8
E9
E10
E11
E12
E13
E14
E15
E16
E17
E18
E19
E20
E21
E22
E23
E24
E25
E26
E27
E28
E29
E30
P1
O1
O2
O3
1
0.8
0.6
0.4
0.2
0
-0.2
-0.4
-0.6
-0.8
-1

List of Tables

Table 1. Evolution of 'Granny Smith', 'Opal®' and 'Royal Gala' apples during on-tree development, indicating the date and days after full bloom (DAFB) at each sampling point.

Sampling point	S1	S2	S3	S4	S5	S6*
Sampling date	May 27th	June 22nd	July 17th	August 15th	Sept. 10th	Oct. 1st Sept. 27th
Granny Smith	45 DAFB	71 DAFB	96 DAFB	125 DAFB	151 DAFB	172 DAFB
Opal®	50 DAFB	76 DAFB	101 DAFB	130 DAFB	156 DAFB	173 DAFB
Royal Gala	45 DAFB	71 DAFB	96 DAFB	125 DAFB		

* The sampling point S6 corresponded to October 1st for 'Granny Smith' and September 27th for Opal®

Table 2. Apple quality parameters at harvest (CHD corresponds to sampling points S4 in 'Royal Gala' and S6 in 'Opal®' and 'Granny Smith') and at the sampling point previous harvest (Pre-CHD corresponds to sampling points S3 in 'Royal Gala' and S5 in 'Opal®' and 'Granny Smith'). Data shown are means ± standard error. Capital letters indicate significant differences between Pre-CHD and CHD for each cultivar according to Student's t-test ($P < 0.05$). Lowercase letters indicate significant differences among cultivars at each sampling point according to Tukey test ($P < 0.05$).

Parameter	Sampling Point	Cultivar					
		Royal Gala		Opal®		Granny Smith	
Firmness (N)	Pre-CHD	106 + 1.2	A, a	84 + 1.2	A, b	88 + 1.1	A, b
	CHD	76 + 1.5	B, ab	74 + 0.6	B, b	79 + 1.2	B, a
Starch Index	Pre-CHD	1 + 0.0	B, c	6 + 0.5	B, a	3 + 0.5	B, a
	CHD	7 + 0.7	A, a	8 + 0.3	A, a	5 + 0.3	A, b
SSC (ºBrix)	Pre-CHD	9.0 + 0.63	B, b	13.9 + 0.13	B, ab	10.4 + 0.16	B, a
	CHD	12.1 + 0.07	A, ab	14.5 + 0.09	A, a	11.0 + 0.19	A, b
TTA (g/L)	Pre-CHD	3.8 + 0.12	A, b	5.4 + 0.23	A, a	6.4 + 0.47	a
	CHD	2.7 + 0.05	B, c	4.5 + 0.1	B, b	5.6 + 0.06	a
SSC/TTA	Pre-CHD	2.4 + 0.04	B, ab	2.6 + 0.04	B, a	1.7 + 0.04	b
	CHD	4.5 + 0.03	A, a	3.2 + 0.02	A, b	2.0 + 0.01	c

Supplementary Table S1: Primers used in the present study.

Primer name	Gene	Primer sequence (5' – 3')
MdACS1-Fw	*MdACS1*	CTCCTCCTTTCCTTCGTTGA
MdACS1-Rv		ACCATGTCGTCGTTGGAGTAG
MdACS3-Fw	*MdACS3*	CGAGTTGGCACTGTGTACTCTTA
MdACS3-Rv		ATAACATGGAAGCCAAGAGATGT
MdACO1-Fw	*MdACO1*	ATCAATGATGCTTGTGAGAACTG
MdACO1-Rv		GGTCTTCTTGTAGTGATCCTTGG
MdERF1-Fw	*MdERF1*	TCCAGACCGGTTCTTACTATTAT
MdERF1-Rv		CAGCATCCACAGGTACAAC
MdERF2-Fw	*MdERF2*	TAAAATTGGCAGCAACGCCA
MdERF2-Rv		GTGGGCTCGTGACTTTCGTTA
MdERF3-Fw	*MdERF3*	TGGAAATGGGAGCAGGGATG
MdERF3-Rv		ATTACAGCGTCCTCCGCAAC
MdETR1-Fw	*MdETR1*	CATTTCTCACTTGTCAGGCATGTA
MdETR1-Rv		CAATTCATCAGCCGGCCATT
MdARF2-Rv	*MdARF2*	GTTAAGGCGGCATGCAGATG
MdARF2-Fw		TTGGCAACCAACTCCTGTGT
MdARF4-Fw	*MdARF4*	AATGTCCAGCTGCTTGCTAAC
MdARF4-Rv		TAGGTGATCCTCCATCCCCC
MdARF5-Fw	*MdARF5*	GCTCTTTCCTCCGCTGGATT
MdARF5-Rv		TCCAGTTGTGAGAAGGTGTCG
Md8282-Fw	Reference gene	CTCGTCGTCTTGTTCCCTGA
Md8282-Rv		GCCTAAGGACAGGTGGTCTATG

https://dspace.org/

Cultivar differences in the hormonal crosstalk regulating apple fruit development and ripening: Relationship with flavour components and postharvest susceptibility to Penicillium expansum

Fernández-Cancelo, Pablo; Echeverria, Gemma; Teixidó, Neus; Alamar, M. Carmen; Giné-Bordonaba, Jordi

2023-11-01
Elsevier
https://doi.org/10.1016/j.postharvbio.2023.112532
Fernández-Cancelo P, Echeverria G, Teixidó N, et al., (2024) Cultivar differences in the hormonal crosstalk regulating apple fruit development and ripening: relationship with flavour components and postharvest susceptibility to Penicillium expansum. Postharvest Biology and Technology, Volume 205, November 2023, Article number 112532

Downloaded from a DSpace repository. https://dspace.org/